Boletín de la Sociedad Geológica del Perú

journal homepage: www.sgp.org.pe ISSN 0079-1091

The Eocene-Oligocene Otuma Depositional Sequence (East Pisco Basin, Peru): Paleogeographic and Paleoceanographic Implications of New Data

Thomas J. DeVries[1], Mario Urbina[2], and Nathan A. Jud[3]

[1]Burke Museum of Natural History and Culture, University of Washington, Seattle, Washington 98195, USA. Corresponding address: Box 13061, Burton, Washington 98013 USA (tomdevrie@aol.com)
[2]Departamento de Paleontología de Vertebrados, Museo de Historia Natural Javier Prado, Universidad Nacional Mayor de San Marcos, Lima, Peru
[3] L. H. Bailey Hortorium, Plant Biology Section, School of Integrative Plant Science, Cornell University, Ithaca, New York 14853, USA (nathan.jud@cornell.edu)

ABSTRACT

The Otuma depositional sequence (East Pisco Basin, southern Peru) comprises late Eocene basal mollusk-bearing sandstones and overlying silty sandstones with pelagic microfossils and clupeoid fish scales. Field work conducted over the course of thirty years has provided strong evidence that the youngest Otuma sediments pass into the early Oligocene. Scoured horizons at mid-section with pebbly bioclastic sandstone or glauconitic sandstone and mudstone may represent global events of rapidly falling sea level associated with the Eocene-Oligocene Transition. Lithologic, stratigraphic, and paleontological data are used to reconstruct for Otuma time the paleogeography of the East Pisco Basin, characterized by a northern archipelago separated from a central embayment and southern open coast by a peninsula at the latitude of Ica. Faunal lists of Otuma mollusks and vertebrates are updated, gathering together published and unpublished accounts of giant Eocene penguins, pelagornithid birds, gavialoid crocodiles, and the archeocete, *Cynthiacetus*. The first detailed account is presented of fossil wood from the East Pisco Basin: a fragment of a large legume tree trunk, one of many that were stranded in the central embayment during a late progradative phase of Otuma deposition.

RESUMEN

La secuencia deposicional Otuma (Cuenca Pisco Este, sur del Perú) comprende areniscas basales con moluscos del Eoceno tardío recubiertas por areniscas limosas con microfósiles pelágicos y escamas de peces clupeoideos. El trabajo de campo ha proveído de fuerte evidencia que los sedimentos más recientes de la formación Otuma sobrepasan hacia el Oligoceno temprano. Los horizontes de erosión en la sección media, con una secuencia de guijarros de arenisca bioclástica, arenisca glauconítica y limo podrían representar eventos globales de una rápida caída en el nivel del mar asociado con la transición Eoceno-Oligoceno. Se han usado datos litológicos, estatigráficos y paleontológicos para reconstruir paleogeográficamente la Cuenca Pisco Este en los tiempos del Otuma; caracterizada por un archipiélago hacia el norte, una bahía central y la costa abierta al sur, interrumpida por una peninsula en la actual latitud de Ica. Las listas de fauna de moluscos y vertebrados de la formación Otuma han sido actualizadas, juntando información publicada e inédita sobre la presencia de restos de pingüinos gigantes del Eoceno, aves pelagorrnítidas, cocodrilos gavialoideos, y el arqueoceto, *Cynthiacetus*. Se presenta el primer registro detallado de madera fósil de la Cuenca Pisco Este; un fragmento de un gran árbol leguminoso, uno de los varios que fueron varados en el ensenamiento durante una fase progresiva de la deposición Otuma.

Palabras claves: Eocene, Oligocene, Peru, East Pisco Basin, Otuma Formation, stratigraphy, paleontology.

1. Introduction

The Otuma Formation, provisionally named by DeVries (1998), encompasses marine strata in the East Pisco Basin of southern Peru (Figure 1A) that are referred to a single depositional sequence. The lower bounding unconformity is usually underlain by silty marine sandstone of the Yumaque Member of the Paracas Formation, whereas the upper bounding unconformity is most often overlain by coarse-grained marine sandstone of the Chilcatay Formation. The age of Otuma sediments was first thought to be early Oligocene (DeVries, 1998), but subsequent discoveries of biostratigraphically useful mollusks (DeVries, 2004) and microfossils (DeVries et al., 2006) led to a revised age of late Eocene.

Field work conducted since 2006 has identified additional outcrops of Otuma strata, including exposures across an expansive pampa at the northwestern end of the Gran Tablazo de Ica. New geological data have revealed the varied nature of Otuma lithofacies and permitted a reconstruction of coastal paleogeography in the East Pisco Basin during the late Eocene and early Oligocene.

In addition to introducing new data, this report reiterates and in some cases re-interprets radiometric and paleontological data that first appeared in abstract form (DeVries, 2004, DeVries et al, 2006). Evidence is presented of a mid-sequence shoaling event that may correspond to falling sea level during the Eocene-Oligocene Transition (EOT) (Miller et al., 2005). An updated list of Otuma mollusks is given; a diverse assortment of Otuma penguins, sharks, crocodiles, and archeocetes is noted; and the first published account of fossil wood in the East Pisco Basin is presented.

2. Methods and Materials

Field work between 1986 and 2016 has consisted of measuring sections, describing lithology and sedimentary structures, and understanding the relationships between fossils, lithofacies, and paleo-shorelines, the interplay of which has produced a paleogeographic reconstruction for Otuma time imbued with paleoecological detail. Field localities were once marked on 1:100,000 quadrangle maps but later were plotted using GPS coordinates (Appendix). Localities with a "DV" designation are those of the senior author. Localities with a "JM" designation were visited during the 1980s by José Macharé (Macharé, 1987; Macharé and Fourtanier, 1987).

Absolute ages derived from ^{40}Ar-^{39}Ar data have been provided by Larry Snee (United States Geological Survey, Denver, Colorado, retired), the Servicio Nacional de Geología y Minería de Chile, and Kevin Nick (Loma Linda University, California, USA). Microfossils used for biostratigraphy from unpublished and abstracted sources have included diatoms, identified in the 1980s by John Barron (United States Geological Survey, Menlo Park, California, USA) and Hans Schrader (University of Bergen, Norway, retired) and more recently by Pedro Tapia (Universidad Cayetano Heredia, Lima), and radiolarians and nannofossils, identified by the late Yanina Narváez (DeVries et al., 2006) and more recently by Elisa Malinverno (Dipartimento di Scienze dell'Ambiente e del Territorio e di Scienze della Terra, Università degli Studi di Milano-Bicocca, Milan, Italy).

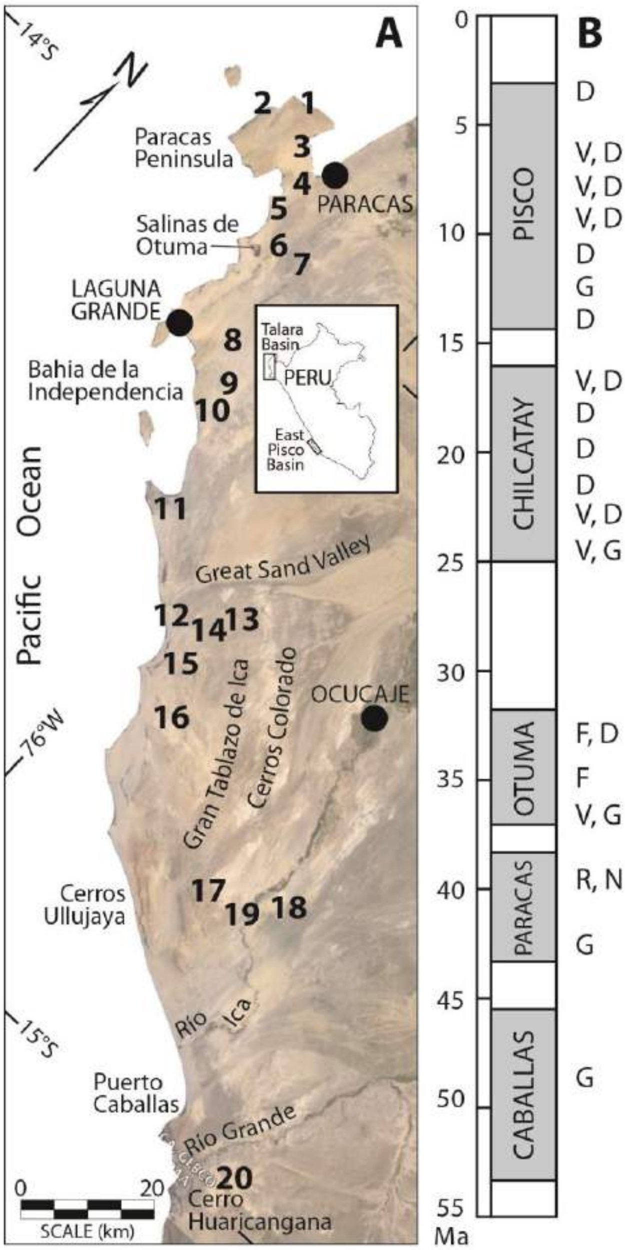

__Figure 1.__ Localities and stratigraphy of the East Pisco Basin. A. Map showing the locality of the East Pisco and Talara basins in Peru and outcrop areas in the East Pisco Basin. 1–Playa Talpo, 2–Playa Los Viejos, 3–Necropolis. 4–type locality of Otuma Formation (DeVries, 1998), 5–Playa Yumaque Southeast, 6–Pampa Las Salinas, 7–Cerro Santa Cruz, 8–Cerro Sombrero, 9–Cuenca Sombrero, 10–Carhuas-Comotrana Road, 11–Morro Quemado East, 12–Palo Vento Passes, 13–Pampa Concha Roja, 14–Pampa Negra, 15–Bajada del Diablo / Camino de los Burros, 16–Quebrada Perdida, 17–Cerro Tiza, 18–Samaca East, 19–Samaca West, 20-Quebrada Huaricangana. B. Stratigraphic column showing unconformity-bound depositional sequences (and eponymous formations) for the East Pisco Basin. Data from DeVries (1998, 2004) and DeVries et al. (2006), an unpublished radiometric age from the uppermost Chilcatay Formaton (K. Nick, 23 May 2016, written communication), and this report. Radiometric and biostratigraphic data are referenced by letters to the right of the column. D=diatoms, F=foraminifera, G=gastropods, N=nannofossils, R=radioalarians, V=volcanic ash and ^{40}Ar-^{39}Ar datations.

Fossil wood samples were identified by one of the authors (Nathan A. Jud). Vertebrates were identified by another author (Mario Urbina), Rodolfo Salas-Gismondi (Departamento de Paleontología de Vertebrados, Museo de Javier Prado, Universidad Nacional Mayor de San Marcos, Lima, Peru), and Ali Altamirano, formerly with the aforesaid museum. Mollusks were identified by the lead author and compared with published Eocene and Oligocene faunas of northern Peru (Woods, 1922; Olsson, 1928, 1930, 1931) and the East Pisco Basin (Lisson, 1925; Rivera, 1957). Fossil mollusks and vertebrates have been deposited with the Departamento de Paleontología de Vertebrados in Lima.

3. Previous Work

Rivera (1957) was the first to call attention to strata now assigned to the Otuma Formation, but only as a discrete biostratigraphic unit, the *Turritella woodsi* Zone. Her perception of the contiguity of turritelline beds with silty sandstone of the Paracas Formation (the Yumaque Member, in current parlance (Dunbar et al., 1990; DeVries, 1998)) and crystalline basement rock was sometimes incorrect because she did not recognize the effects of faulting. Nonetheless, Rivera (1957) correctly placed the turritelline beds atop the Eocene section in the East Pisco Basin and, based on mollusks that she identified and foraminifera identified by Dora Guiterrez (Newell, 1956), correlated the uppermost "Paracas" beds with the Chira Formation of northern Peru's Talara Basin, deemed then and now (Hanna and Israelsky, 1925; Olsson, 1931; Higley, 2004; Narváez and Pardo-Arguedas, 2009) to have a late Eocene age.

DeVries (1998) defined a lithostratigraphic unit, provisionally termed the Otuma Formation, which encompassed the *T. woodsi*-bearing beds of Rivera (1957) and superjacent silty marine sandstone. Based on diatom, nannofossil, and foraminiferal data (Macharé and Fourtanier, 1987; Stock, 1990; Ibaraki, 1993), constrained by $^{40}Ar/^{39}Ar$ ages of 37.2, 36.5, and 35.7 Ma in presumed upper Yumaque beds at Samaca West, and consistent with the occurrence of the temporally wide-ranging *Turritella woodsi* Lisson, 1925, DeVries (1998) assigned an early Oligocene age to the Otuma sequence.

The discovery of a diverse molluscan assemblage in basal Otuma sediments at Bajada del Diablo and Cerro Santa Cruz, including several species also known from the Chira/Verdun sequence in the Talara Basin, led DeVries (2004) to revise the age of the Otuma Formation to late Eocene. Further refinement of the age (DeVries et al., 2006) used new radiolarian and nannofossil data and incorporated a revised stratigraphy at Samaca West, which placed the three ^{40}Ar-^{39}Ar-dated ash beds above the Paracas/Otuma unconformity. These new data fixed the age of the lower Otuma Formation as late Eocene.

The age of the uppermost Otuma beds had been constrained by the age of basal transgressive sandstones of the overlying Chilcatay sequence, inferred as latest Oligocene based on radiometric dates obtained near Caravelí (DeVries, 1998). The angular unconformity that exists between the underlying Otuma and overlying Chilcatay sequences coincides with the widespread late Oligocene Aymara tectonic phase (Sébrier and Soler, 1991).

4. Stratigraphic Nomenclature

The existence of the Otuma Formation is still denied in some quarters (Leon et al., 2008), while others have pointed out the difficulty of recognizing the lithostratigraphic unit in the field. Indeed, mapping any of the four exclusively marine Cenozoic formations in the East Pisco Basin (Paracas, Otuma, Chilcatay, Pisco; Figure 1B) is challenging because each is characterized by a transgressive, orange-weathering, medium- to coarse-grained sandstone overlain by white-weathering silty sandstone. Without knowing where in the field the relevant sequence-bounding unconformities are located or what the ages are of mollusks found in transgressive sandstones, recognizing formations underfoot can be a problem.

Criteria for defining formations in the East Pisco Basin have been applied inconsistently. A formation consists of lithologically similar strata that have a continuity that can be mapped over a significant distance (Murphy and Salvador, 2016, Chapter 5). Consequently, each orange transgressive sandstone and each white silty sandstone in the East Pisco Basin could merit formation status. Such an approach was indeed adopted by Dunbar et al. (1990) when they defined the Los Choros Formation (transgressive sandstone) and Yumaque Formation (silty sandstone) as part of a Paracas Group. The same nomenclatural logic, however, was not applied to the Chilcatay or Pisco formations.

Attaching a formation name to each transgressive sandstone in the East Pisco Basin poses a special difficulty. The transgressive sandstones, often indistinguishable except for the fossil species they contain (information that, according to guidelines in Chapter 10 of Murphy and Salvador (2016), cannot be used to define a lithostratigraphic unit), can be contiguous with one another. This happens near the Paracas Peninsula, where Otuma sandstone overlies Paracas sandstone (DV 1142, 1145), and in the Río Ica valley, where Chilcatay sandstone overlies Otuma (DV 7162) or Paracas sandstone (DV 7036). Based on the criteria of lithologic similarity and mappable continuity, these couplets of temporally disjunct sandstones could merit single formational appellations.

The alternative to defining a formation in the East Pisco Basin is to define a sequence, i.e., "a relatively conformable succession of genetically related strata bounded at its top and base by unconformities or their correlative conformities" (Mitchum et al., 1977) or a depositional sequence (Catuneanu et al., 2011). In the sediment-starved forearc basins of central Peru, the progradational/basin-offlap phase emphasized by Galloway (1989) is usually absent. Basal transgressive beds in the East Pisco Basin are underlain by a planar, erosional nonconformity (Figure 2A), angular unconformity (Figure 2B), or disconformity (Figure 2C). The erosional surface is usually incised in silty sandstone of the preceding sequence (Figures 2C, 2F), the result of a forced regression (Catuneanu et al., 2011). *Ophiomorpha* burrows may mark the horizon.

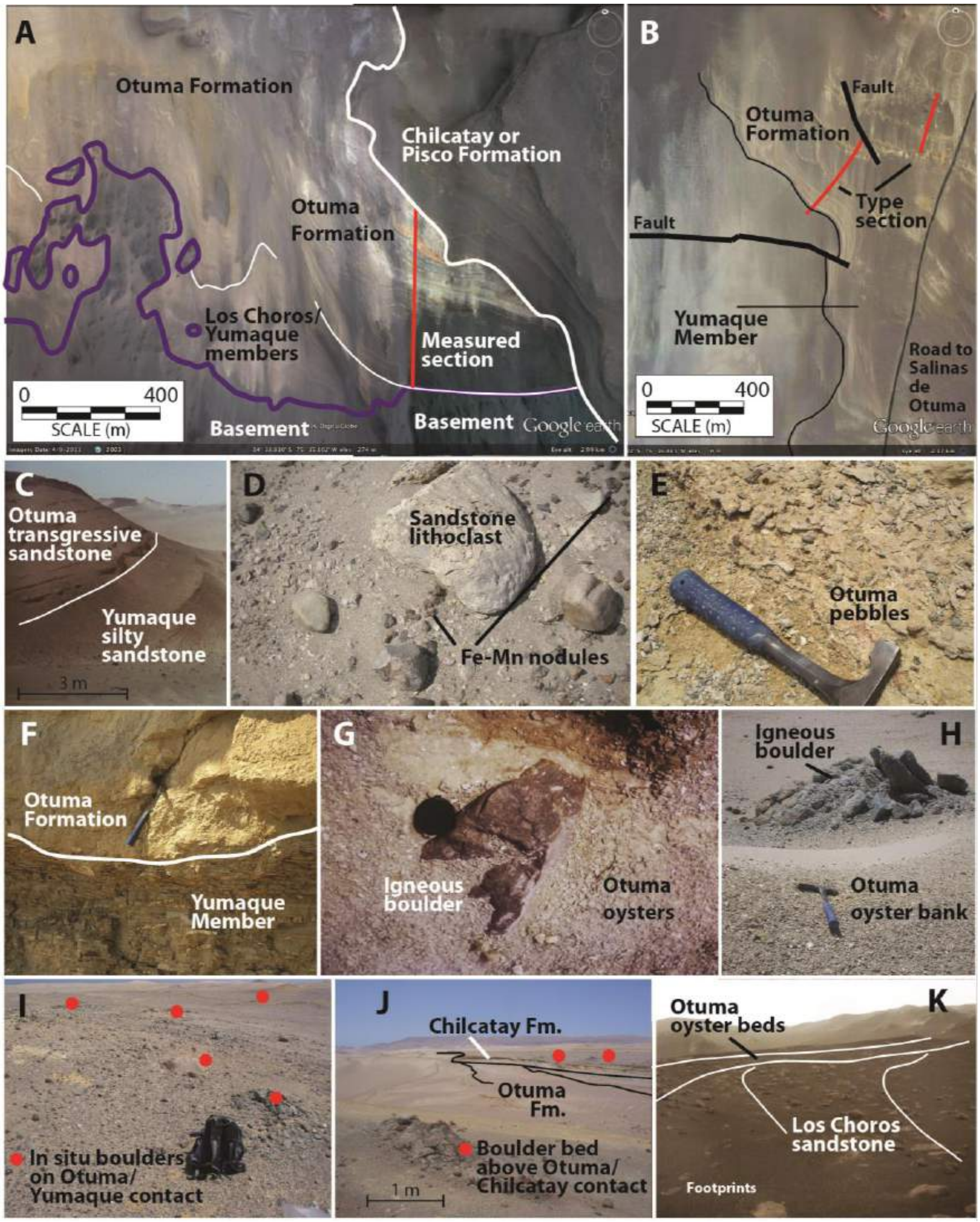

Figure 2. *Lower sequence boundaries of Otuma (A-I, K) and Chilcatay sequences (J). A. Google Earth base map with Cenozoic outcrop shown on eastern side of Samaca East. Purple line=limit of basement, thin white line=disconformable base of Otuma sequence, thick white line=angular unconformable base of Chilcatay sequence. Nonconformable base of Otuma sequence is where purple and white lines overlap at base of measured section at DV 7161. B. Google Earth base map of type section of Otuma Formation in angular unconformity with underlying Yumaque Member. C. Disconformable contact at DV 1441 with shallow-water Otuma sandstones overlying deeper-water Paracas silty sandstones – a forced regression. D. Manganese-iron nodules and lithoclasts at base of Otuma sequence 300 meters northeast of DV 1903. E. Basal pebbly sandstone of Otuma sequence. F. Basal bioclastic sandstone of Otuma Formation overlying silty sandstone of Yumaque Member at DV 502. G. Boulder in Turritella woodsi-bearing sandstone, base of Otuma sequence near the Necropolis at DV 818. H. Large boulder of crystalline basement rock on Yumaque-Otuma contact along Carhuas-Comotrana Road at DV 1815. I. Small boulders of granite scattered along Yumaque-Otuma contact in the Cuenca Sombrero at DV 1172 and DV 1173. J. Intraformational boulder beds in transgressive sandstone of Chilcatay sequence at Samaca West at DV 508. K. Angular unconformity separating contiguous transgressive sandstones of Paracas and Otuma sequences at DV 1142 and DV 1145.*

Where the underlying beds, often dolomitized, are semi-lithified, they may be bored on their upper surfaces or contain *in situ* pholad bivalves.

Lower sequence-bounding unconformities in the East Pisco Basin are covered by either a veneer of bioclasts and nodules – manganese, iron, phosphate, abraded bones, shark teeth, and fragments of barnacles and bivalves (Figure 2D) – or medium- and coarse-grained bioclastic sandstone and gravel (Figures 2E, 2F), in some cases with cobbles or boulders of crystalline rock (Figures 2G, 2H, 2I) or lithoclasts (Figure 2D), some of which exceed one meter in diameter (Figure 2H).

Since authigenic precipitates do develop on non-depositional surfaces within sequences in the East Pisco Basin and since intra-sequence horizons with cobbles, boulders, and transported shallow-water bioclastic debris (Figure 2J) do exist, reliably identifying a lower bounding sequence boundary in the East Pisco Basin requires evidence of forced regression, preferably accompanied by evidence of tectonic or phylogenetic events that imply an extended period of time.

5. Results

5.1. Stratigraphy

Outcrops of Otuma sediments reported since 1998 included sections at Cerro Santa Cruz and Bajada del Diablo / Camino de los Burros (DeVries, 2004), Quebrada Perdida, the northwestern Gran Tablazo de Ica, and Samaca East (DeVries et al., 2006) (Figure 1A). All have been revisited since 2006. In addition, new areas of Otuma outcrops have been studied at Playa Yumaque Southeast, Cuenca Sombrero, Pampa Negra, the Palo Vento Passes, and the eastern edge of Samaca East (Figure 1A). The following geological and paleontological data are presented by outcrop from north to south.

5.1.1. Playa Yumaque Southeast

Playa Yumaque, the type locality for the Yumaque Member of the Paracas Formation, is structurally complex. Fault-bound blocks with Otuma sandstone (DV 2036-2046) containing oysters, the bivalve, *Cardita newelli* Rivera, 1957, and concentrations of *T. woodsi* are interspersed with blocks composed largely of Paracas strata (DV 839, 2038) with dispersed specimens of *Turritella lagunillasensis* Rivera, 1957. At localities DV 2040 and DV 2041, a steel-gray coarse-grained sandstone underlies *T. woodsi*-bearing sandstone and marks the base of the Otuma sequence; it is associated with an *in situ* 80-cm-diameter igneous boulder, ramose bryozoans, oyster valves, and a specimen of the bivalve, *Crassatella pedroi* DeVries, 2016. Nearby, an ash bed a few centimeters beneath a *T. woodsi*-bearing bed (DV 2036) has an ^{40}Ar-^{39}Ar age of 35.9 ± 0.3 Ma (P. Baby, 8 April 2016, written communication).

On cliffs facing Playa Supay, two kilometers south of Playa Yumaque, two localities, one (DV 2038) with a few specimens of the turritelline gastropods, *T. lagunillasensis* and *Cristispira paracasensis* (Rivera, 1957), the other (DV 2039) with abundant *T. woodsi*, exemplify the juxtaposition of blocks of Paracas and Otuma sediments. A foram assemblage with *Pseudohastigerina micra*, *Cassigerinella chipolensis*, and *Chiloguembelina cubensis* described by Ibaraki (1993) from Playa Supay (sample Pe-88-6-1) is inferred to come from Otuma beds. The species indicate an assignment to the *Cassigerinella chipolensis*/*Pseudohastigerina micra* Concurrent Range Zone of Bolli and Saunders (1985), equivalent to Blow's (1969) planktonic foraminiferal zones P18 and P19, Berggren and Miller's (1988) renamed *Chiloguembelina cubensis*/ *Pseudohastigerina* spp. Partial-range Zone (= a redefined P18 Zone), Berggren et al.'s (1995) *Turborotalia cerroazulensis*-*Pseudohastigerina* spp. Interval Zone (estimated age: 33.8-32 Ma), and Berggren and Pearson's (2005) *Pseudohastigerina naguewichiensis* Highest-occurrence Zone (estimated age: 33.7-32 Ma, i.e., early Oligocene).

5.1.2. Pampa Las Salinas and Cerro Santa Cruz

Outcrops at Pampa Las Salinas and Cerro Santa Cruz discussed by DeVries (1998, 2004) warrant further comment. Two kilometers offshore (west) of a late Eocene shoreline punctuated by sea stacks of igneous rock, sandstone beds occur with 20-cm-long oyster valves, cobbles, and 80-cm-diameter igneous boulders and are overlain by beds packed with *T. woodsi* (DV 842). One kilometer closer to the Eocene shoreline (DV 1142, 1143, 1144), basal fossiliferous beds are overlain by a unit of red rounded cobbles of granite, evidently sourced from western basement outcrops. The cobble horizon is overlain by sandstone beds with abundant oyster valves and shells of *T. woodsi*. These fossiliferous beds continue eastward to within one-half kilometer of the Eocene shoreline, but closer (DV 404, 1160), only the oyster valves remain, joined by small *Chlamys* and mytilid bivalves in a pebbly sandstone. At locality DV 1161, primary gypsum and crinkly bedded marl suggestive of microbial laminites (Palma et al., 2013) indicate the former presence of a brackish lagoon similar to a Pleistocene pantano near Sacaco described by Salas et al. (2004). At the Eocene shoreline, (DV 405, 415, 1146, 1148, 1149, 1150), bioclastic sandstones and coquinas with oysters, mytilids, barnacles, and sea urchin spines wrap around the Eocene sea stacks.

Below the Otuma beds and in angular unconformity with the basal Otuma beds (Figure 2K) are medium- and coarse-grained transgressive sandstone beds of the Los Choros Member of the Paracas Formation (DV 1142), which near the Eocene sea stacks becomes coarser-grained with granules of black igneous rock, oyster valves, and sea urchin spines (DV 1145). In such close proximity to the Eocene shoreline, on-lapping beds of the Los Choros and Otuma formations are lithologically indistinguishable.

Higher in the section, above the boulders, shell beds, and evaporites, are medium-grained sandstones (DV 1144, 1151, 1152, 1153) with a more diverse molluscan assemblage that still includes *C. newelli* and *T. woodsi*. The most diverse assemblage occurs at Cerro Santa Cruz (DV 1154, 1402) where the occurrence of *Turritella cochleiformis* (Gabb, 1869), *Ficus chiraensis* Olsson, 1931, *Ectinochilus gaudichaudi* (d'Orbigny, 1842), and *Peruchilus culberti* Olsson, 1931, indicate a correlation of the lower Otuma sequence with the upper Eocene Chira-Verdun Formation of the Talara Basin in northern Peru (DeVries, 2004; Narvaez and Pardo-Arguedas, 2009).

In fine-grained deposits from higher in the Otuma sequence (Pe-88-7-11, approximately equivalent with DV 842), Ibaraki (1993) encountered *Tenuitella insolita* (= *Globorotalia insolita*; see Pearson et al., 2006), the nominate foram species of the *Tenuitella insolita* Taxon-range Zone, with a late Eocene age range of 35.5 to 34.4 Ma (Huber and Quillivere, 2005), older than the early Oligocene age (Zone P21a) proposed by Ibaraki (1993). The occurrence of the wider ranging (*Chiloguembelina cubensis* (late Eocene to late Oligocene; Pearson et al., 2006) and *Paragloborotalia opima* (Eocene to Oligocene; Bolli and Saunders, 1985) in Pe-88-7-11 and two nearby samples (Pe-90-7-3, Pe-90-7-4; Ibaraki, 1993) do not further constrain the age of these samples.

Diatoms samples (83JM 104 and 83JM 062; Macharé and Fourtanier, 1987) from the fine-grained Otuma sediments on Pampa Las Salinas include *Distephanosira architecturalis* (= *Melosira architecturalis*; see Fenner (1985) and Glezer et al. (1992)), *Hemiaulus polycystinorum*, *Skeletonema barbadense*, and *Thalssiosira mediaconvexa*, species characteristic of the middle and/or late Eocene (Bolli and Saunders, 1985). Sample 86JM 060, however, contains *Rouxia obesa*, a species associated with the early Oligocene (Gombos and Ciesielski, 1983; Bolli and Saunders, 1985; Baldauf, 1992).

5.1.3. Cerro Sombrero and Cuenca Sombrero

The name "Cerro Sombrero" is informally applied to an isolated hill of igneous rock seven kilometers northeast of Laguna Grande. Four meters of coarse-grained gravelly sandstone with typical Otuma mollusks (a basal coquina of *C. newelli* overlain by sandstone with *P. culberti*, oysters, and venerids; DV 1112, 1122, 1123) are separated by an angular unconformity from underlying chocolate-brown foram-rich silty sandstone (Yumaque Member) and in turn are overlain with silty sandstone containing forams and clupeoid fish scales.

"Cuenca Sombrero" informally refers to a basin four kilometers southeast of Cerro Sombrero. On the floor of the basin are fossiliferous sandstone beds of the Los Choros Member (DV 1819, 3013a, 3015). The base of the Otuma depositional sequence is marked along an arcuate contact (from east to west, DV 4005, 1220, 1221, 1222, 1172, 1173, 1913) by scattered angular boulders of crystalline basement rock (Figure 2I) and coarse-grained sandstone with a diverse fauna of Otuma mollusks (*Bursa chira* Olsson, 1930; *P. culberti*, *T. woodsi*, *Xenophora carditigera* Nielsen and DeVries, 2002; *C. newelli*, oysters, venerids). The transgressive sandstone overlies silty sandstone of the Yumaque Member and is overlain by tuffaceous silty sandstone with forams, diatoms, and clupeoid fish scales. Nannofossils (*Cribrocentrum reticulatum, Reticulofenestra bisecta, Sphenolithus radians*) from the upper silty sandstone (DV 1171-1, 1173-5) confirm a late Eocene age for the lower Otuma sequence (DeVries et al., 2006), older than the top of zone NP 19/20, or 34.5 Ma for *C. reticulatum*. Nannofossils from the underlying Yumaque silty sandstone (DV 1173-3; *Chiasmolithus solitus, Reticulofenestra umbilicus*) indicate an age of middle Eocene, within zone NP 16, i.e., about 43 to 40 Ma (DeVries et al., 2006).

5.1.4. Carhuas-Comotrana Road

A measured section of the Otuma Formation north of the Carhuas-Comotrana Road (DV 631) was described by DeVries (1998). The base of the Otuma sequence is defined by a pebbly conglomerate with iron-manganese-phosphate nodules and specimens of *C. pedroi*, oysters, and small gastropods. Overlying the basal pebble lag are ten meters of a fining-up sequence of sandstone with mollusks (*C. newelli*, *Corbula* sp., *P. culberti*, *X. carditigera*) and trace fossils (*Gyrolithes*). One kilometer to the east (DV 5023), closer to the Eocene shoreline, the basal bed includes boulders of igneous rock as well as coarse-grained sandstone and oysters. Three kilometers to the south (DV 632, 1815, 2259, 2260), close to extensive outcrops of crystalline basement rock, the Otuma base consists of densely packed oyster coquina and granite boulders as large as two meters in diameter (Figure 2H). Sandstone beds above the oyster coquina contain *C. newelli*, *P. culberti*, and *X. carditigera*. A siltstone bed (DV 631-9) overlying the transgressive sandstone by just six meters contains the nannofossil species complex *Reticulofenestrata reticulata* + *R. bisecta* (E. Malinverno, 22 June 2016, written communication), indicating an age between 40.0 and 34.4 Ma (Young et al., 2016). The same sample includes the diatoms *Distephanosira architecturalis* and *Rhizosolenia oligocaenica* (= *Rhizosolenia gravida*; see Fenner (1985)) (H. Schrader, 28 January 1991, written communication), indicating an age of about 36 to 33 Ma according to the southern Atlantic Ocean diatom zonation of Gombos and Ciesielski (1983) (see also Baldauf and Barron (1991) and Ramsey and Baldauf (1999)). The entire suite of microfossils, therefore, points to an age of about 36 to 35 Ma for the onset of deep-water Otuma deposition, consistent with radiometric dates on ash beds intercalated with diatomaceous siltstones at Samaca West (see below).

5.1.5. Morro Quemado East

A down-dropped block of Cenozoic marine sandstone surrounded by high bluffs of basement rock lies about eight kilometers east of Morro Quemado. Specimens of venerids and *Cardita* (DV 1136, 1445) point to an Otuma sequence source.

5.1.6. Northwest Gran Tablazo de Ica/Pampa Concha Roja

The Gran Tablazo de Ica extends 30 kilometers northwest from the Río Ica valley. At its farthest reach is a rugged pampa floored by a faulted and tilted section of alternating soft and indurated sandstone. This informally designated "Pampa Concha Roja" is bordered to the northwest by a broad flat-bottomed valley (the "Great Sand Valley"), which is flanked on its northwest side by a 200-meter wall of crystalline basement rock; to the northeast by Miocene strata of Cerros Colorado; and to the south by knobby hills of crystalline basement rock and the half-graben of Playa El Diablo / Camino de los Burros (Figure 1A). The presence of the molluscan taxa, *C. newelli* and *T. woodsi*, establish an Otuma age for the Pampa Concha Roja section.

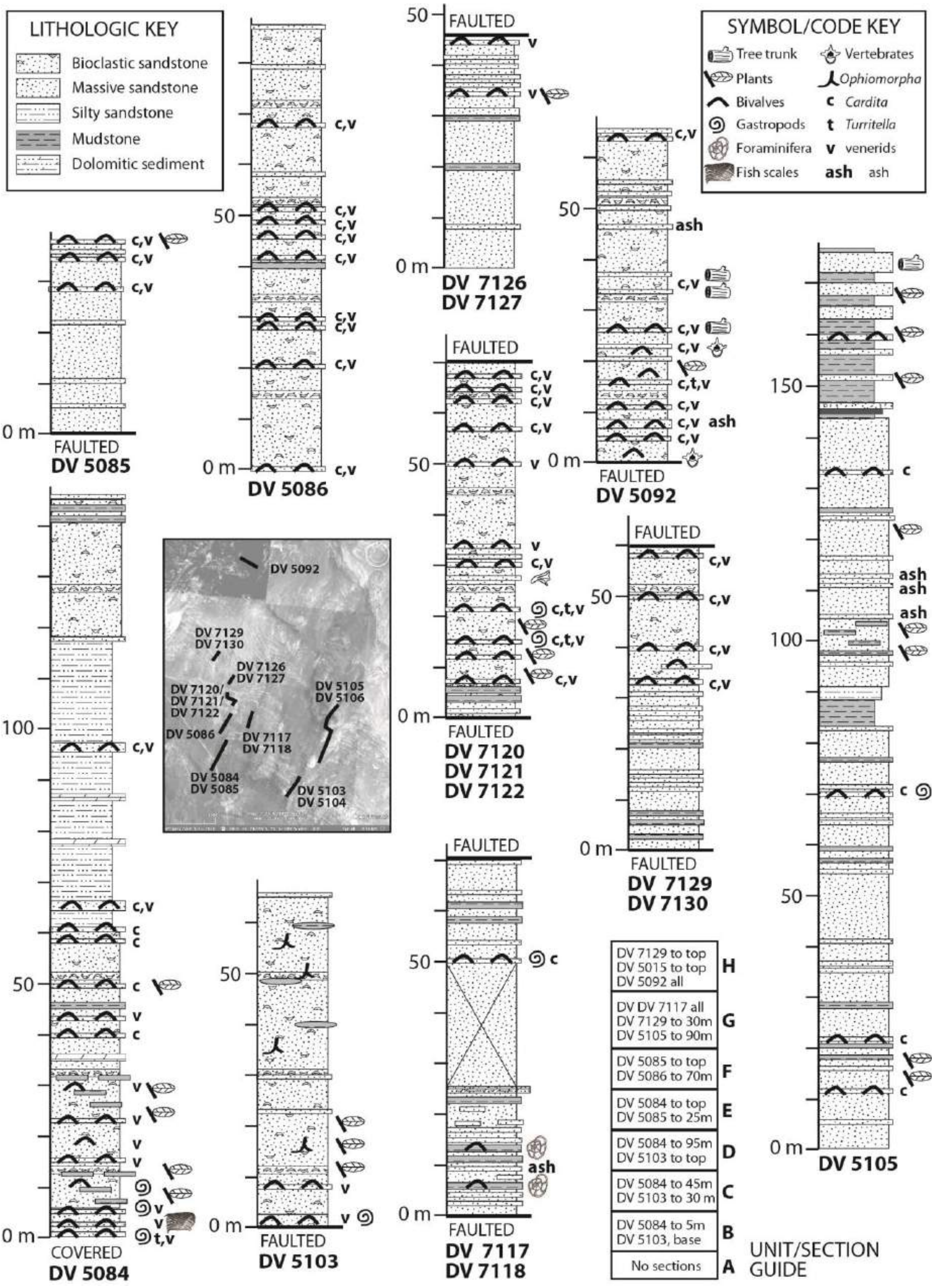

Figure 3. *Stratigraphic sections from Pampa Concha Roja. Successive lithofacies-biofacies units (A-H) described in the text are cross-referenced with sections at lower right. The location of sections on Pampa Concha Roja is shown on a Google Earth base map at center left. There is no intent to tightly correlate one section with another, although the four sections at left are arranged and aligned as approximately correlative sections of the lower Otuma Formation. The same is true for the six sections at right, for the upper Otuma Formation. Two keys are located at the top of the figure, left and right.*

Several short sections were measured on Pampa Concha Roja (Figure 3). The measured sections are reliably ordered in a sequence of units from oldest (A) to youngest (H). Correlation of overlapping sections is less certain. Least certain is the true thickness of the sections, since faults striking close to the bedding strike are likely to produce an undiscerned repetition of the section. Thus, the cumulative section thickness (CST) on Pampa Concha Roja of about 400 meters is likely an overestimate by a factor of two or three. To remedy the situation while still extracting the most information possible, each of the units (A-H) is considered to represent an approximately correct proportion of the entire section without the gross thickness being considered accurate.

The contact of the Otuma sequence with either the Yumaque Member or crystalline basement on Pampa Concha Roja is hidden by alluvium. Outcrops farthest west (Unit A; the oldest of the beds that dip northeast about 12-15 degrees) consist of *Ophiomorpha*-bioturbated medium-grained sandstone with lenses containing *C. newelli* and venerids and horizons with rounded clasts of pumice (DV 7135-7138). One kilometer to the east, the lowest indurated sandstone beds (Unit B), some being channel-form and others having cobbles (DV 3022, 5084, 5101, 5103, 5118), contain a diverse assemblage of Otuma mollusks, including *T. woodsi* and *X. carditigera*, with shell lags of *C. newelli* and venerids.

Overlying sandstones of Unit B are soft-weathering, medium-grained, bioturbated, wood-bearing sandstone beds (Unit C) with interspersed indurated sandstone beds containing concentrations of venerids and *Corbula* (DV 5084, 5103). Beds of Unit C, nominally 40 meters thick, represent ten percent of the CST. Overlying the woody beds of Unit C is a 50-meter interval (Unit D, representing 12 percent of the CST) beginning with a thin bed of mudstone, followed up-section by massive medium-grained sandstone, monospecific lag deposits of *C. newelli*, tuffaceous silty sandstone without fish scales, and a thin bed with pebbles, gravel, and fragments of venerids and *C. newelli* (DV 5084, 5103).

Overlying the pebble sandstone is a nominally 70-meter-thick section (Unit E), 17 percent of the CST, with closely spaced thin- and medium-bedded beds of indurated sandstone and few bivalves (DV 5084, 5085). Marking the beginning of "Unit F" is a thick bed with densely packed venerids and *C. newelli* (DV 3022, 5085, 5086), a pair of bivalve taxa that are dominant in lag deposits interbedded in the overlying 70 meters (17 percent of the CST). Overlying the beds of Unit F are 100 meters (25 percent of the CST) of thin beds of indurated mudstone or sandstone intercalated with soft-weathering, medium-grained, woody sandstone or mudstone with tiny bivalves (*Nucula*, mactrids) but without fish scales (Unit G). Shell lags of *Cardita* and venerids are rare.

The upper part of the sequence (Unit H) consists of about 70 meters (17 percent of the CST) of tuffaceous medium-grained sandstone (DV 5105, 7117, 7118, 7126, 7127, 7129) with shell lags of venerids, oysters, and/or *C. newelli*; beds with concentrations of *T. woodsi*; beds with a diverse molluscan assemblage that includes *T. woodsi* and *Crassatella rafaeli* DeVries, 2016, and discrete ash beds (DV 5092), whose ages between 35 and 39 Ma (K. Nick, 10 March 2016, written communication) indicate reworking of ash from early Otuma time. The shell beds are overlain with varied lenses of tuffaceous sandstone, mudstone, bioclastic sandstone, and ash lapilli, together with numerous tree trunks of a leguminous garapa-like tree, some with and some without borings made by marine bivalves.

5.1.7. Palo Vento Passes

Several valleys drop towards the entrance to Playa Palo Vento from the southern highlands that overlook the Great Sand Valley. In one such valley, the lowest exposed orange coarse-grained sandstones (DV 7143), alternatingly indurated and soft-weathering, contain venerid and arcid bivalves, as well as late Eocene shark teeth, abundant large fragments of wood and cane-like plants, and well-rounded cobbles of pumice. Twenty meters higher in the section (DV 7144), pebbly venerid-bearing sandstone and thick-bedded conglomerates occur with cobbles of crystalline basement rock. The conglomerates are overlain by medium- and coarse-grained sandstone (DV 7142) with venerids and rare specimens of *C. newelli*. One valley to the southwest (DV 7146), greenish-yellow silty sandstone of the Yumaque Member is unconformably overlain by venerid- and wood-bearing orange medium-grained sandstone of the Otuma sequence. On the high walls of both valleys are tuffaceous sandstone that may be part of the upper Miocene Pisco Formation.

5.1.8. Pampa Negra

A section in the northwest corner of the informally named "Pampa Negra" (DV 5109) consists of about 30 meters of coarse-grained sandstone with several beds containing densely packed venerid bivalves and rare specimens of *C. newelli*; these beds overlie silty sandstone of the Yumaque Member. The venerid-bearing transgressive sandstone beds are overlain by silty sandstones with clupeoid fish scales. Venerid-bearing sandstones are also exposed in a separate fault block southward along the western rim of Pampa Negra (DV 5110). Farther south, bioclastic sandstone includes pebbles and small cobbles (DV 5111) and even farther south, large cobbles and angular boulders of granite (DV 5112). The latter locality lies just 300 meters from a range of crystalline basement rock, the backside of the footwall of Bajada del Diablo / Camino de los Burros.

Along the northern and northeastern rim of Pampa Negra, silty sandstone is overlain by a 20-meter unit of glauconitic sandstone-filled *Skolithos* burrows penetrating thin-bedded mudstone (DV 7140), with the unit's base consisting of a 20-cm-thick bed of glauconite sand with one-cm-diameter phosphate nodules (DV 7141).

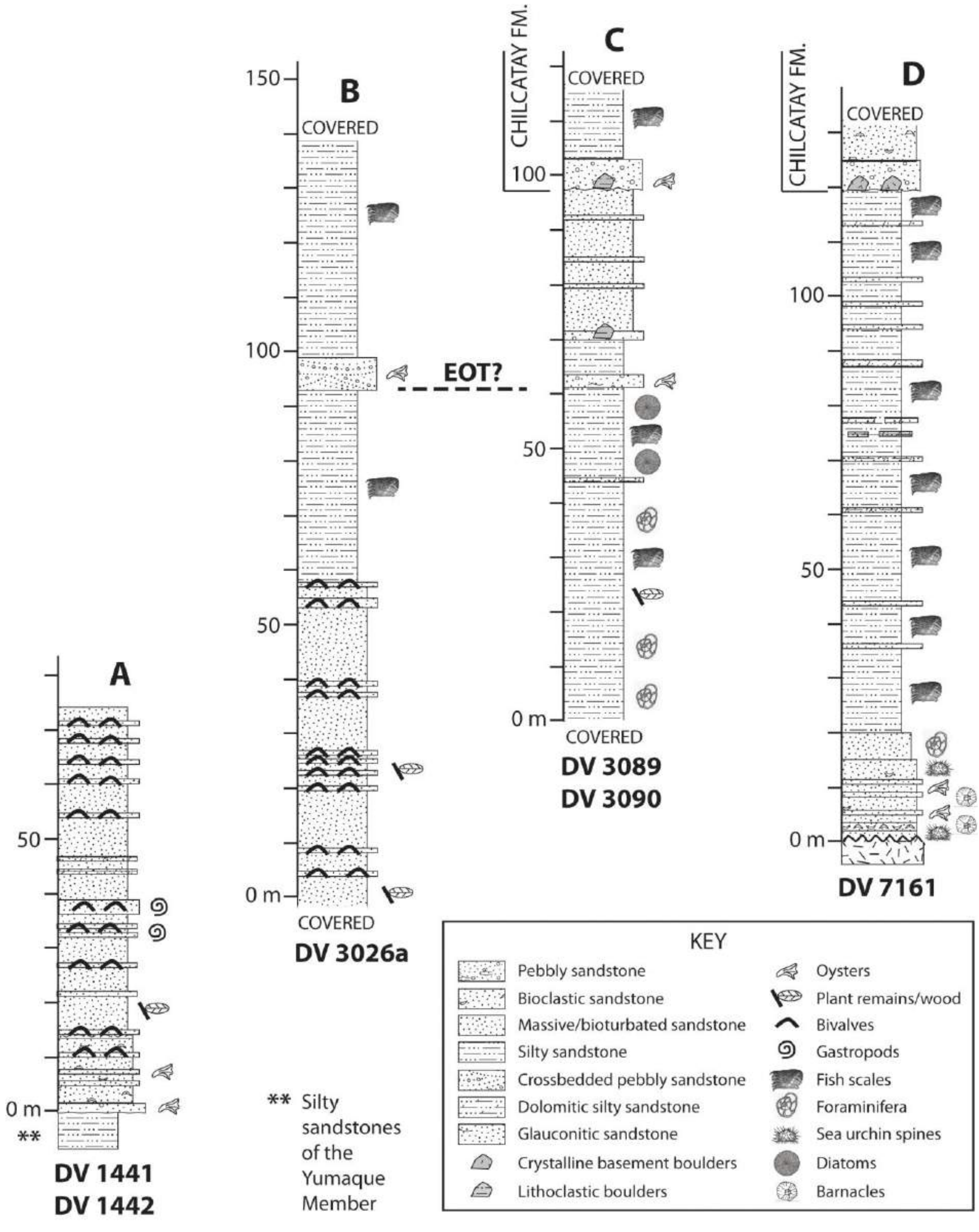

Figure 4. *Stratigraphic sections from the East Pisco Basin. A. Bajada del Diablo, DV 1441/DV 1442. Lower Otuma sequence overlying the Yumaque Member of the Paracas Formation. Transgressive sandstones have a diverse molluscan fauna, including Turritella woodsi and Cardita newelli. B. Camino de los Burros, DV 3026a. Middle to upper Otuma sequence. Late stage transgressive sandstones with venerids and rare Cardita newelli overlain by silty sandstones with pelagic microfossils and clupeoid fish scales. The mid-Otuma shoaling event, possibly correlative with Eocene-Oligocene Transition events of rapidly falling sea level represented by pebbly sandstone between 90 and 100 meters in the measured section. C. Quebrada Perdida, DV 3089/DV 3090. Lower to upper Otuma sequence, base covered. Two mid-Otuma shoaling events may be represented by indurate horizons at 64 and 70 meters in the measured section. The younger of the two events and the basal transgressive sandstone of the overlying Chilcatay sequence with rip-up lithoclasts of dolomitic silty sandstone. D. Samaca East, DV 7161. Lower and middle Otuma sequence. No evidence of mid-Otuma shoaling events below the angular unconformity with the overlying conglomerate of the Chilcatay sequence. Basal invertebrate assemblage of oysters, barnacles, and sea urchin spines is also typical of basal transgressive sandstone of the Los Choros Member of the Paracas Formation.*

5.1.9. Bajada del Diablo/Camino de los Burros

New stratigraphic data from the half-graben of Bajada del Diablo / Camino de los Burros supplements data reported by DeVries (2004). At localities DV 3028 and DV 3029 (also DV 1441-1444), coarse-grained sandstone, gravel, and granite boulders of the Otuma sequence rest disconformably on fine-grained deposits of the Yumaque Member (Figures 2C, 4A). Venerid bivalves and oysters are most common in the lower 20 meters of the Otuma sequence, succeeded in overlying sandstones by a more diverse molluscan assemblage (Table I in DeVries, 2004) that includes *C. newelli* and *T. woodsi*. In the uppermost transgressive sandstones, about 50 meters stratigraphically above the unconformity, molluscan diversity is diminished and *C. newelli* and venerids dominate (DV 1442). Less than two kilometers inland, along the Camino de los Burros (DV 3025, 3026), sandstones with venerids and *T. woodsi* onlap igneous basement rock. A measured section nearby (DV 3026a; see Figure 4B) passes through 60 meters of indurated venerid-packed sandstone beds alternating with softer-weathering sandstone containing dispersed venerid bivalves. Above the venerid-bearing sandstones are five meters of gritty black sandstone and oyster-bearing gravel, overlain by at least 40 meters of silty sandstone.

5.1.10. Quebrada Perdida

The half-graben of Quebrada Perdida has strata of Eocene, Oligocene, and Miocene age rotationally down-dropped to the south, with faults parallel to the master fault and other faults running at right angles, north-south. Bioclastic coarse-grained sandstone of the Los Choros Member with oysters, bryozoans, barnacles, and specimens of *T. lagunillasensis* laps onto basement on the downthrown block of the half-graben (DV 1730, 3060, 3065, 3066, 3067, 3071, 3072). The overlying finer-grained deposits of the Yumaque Member are in turn unconformably overlain by thick-bedded, medium- to coarse-grained, orange sandstone (DV 2219, 2262, 3059) with abundant oysters and specimens of *C. pedroi*, venerids, *P. culberti*, and *X. carditigera*, the same Otuma taxa found across Quebrada Perdida at localities DV 1734 and DV 3076 (the latter also has specimens of *C. newelli*).

Transgressive Otuma sandstone beds in Quebrada Perdida are overlain by 50 meters of brown-weathering, foram-rich, silty sandstone (Figure 4C), which in turn are overlain by 15 meters of white-weathering ash-laden silty sandstone with fewer forams (DV 3089, 3090). Radiolarians (*Artophormis gracilis*, *Cryptocarpium ornatum*, *Lithocyclia aristotelis*, and *Lithocyclia ocellus*) from 10 meters below the base of the white-weathering unit (DV 1731, 1732), incorrectly assigned stratigraphically to the Paracas Formation in DeVries et al. (2006), yield a tightly constrained age of 36.3 to 33.6 Ma. (The presence of the middle Eocene *Lithocyclia ocellus* is thought to represent reworking or contamination.) The disappearance of *C. ornatum* and transition of *L. aristotelis* to *L. angusta*, which define the radiolarian RP19 Zone (Sanfilippo and Nigrini, 1998), occurred at 32.8 Ma, setting the youngest possible age for DV 1732-2. Also, the first occurrence of *A. gracilis* was not at around 36.3 Ma (DeVries et al., 2006), but within the RP20 Zone, i.e., between 32.8 and 28.8 Ma (Nigrini and Sanfilippo, 2001). Whether the older *A. barbadensis* was mistakenly identified in DeVries et al. (2006) as its descendant, *A. gracilis*, can no longer be verified.

The white-weathering Otuma beds are overlain by two distinct 1.5-meter coarse-grained beds, the lower being glauconitic and bioclastic, the upper solely bioclastic and separated from the glauconitic bed by six meters of soft-weathering brown sandstone (DV 3069, 3090, 3092, 3093). The upper bioclastic bed is overlain by 25 meters of brown-weathering silty sandstone. The Otuma sequence is capped by coarse-grained sandstone and conglomerate (DV 3091) containing lithoclasts of dolomitized sedimentary rock and cup-shaped oysters (DV 2213) uniquely associated with the Chilcatay Formation.

5.1.11. Cerro Tiza

The section at Cerro Tiza tilts steeply upward against the fault-bound eastern flank of Cerros Ullujaya. The uppermost sandstone (DV 590, 591) descends northeastward and grades into boulder and conglomeratic beds (DV 1906, 4031, 4032, 4033); its specimens of the muricoid gastropod, *Acanthina katzi* Fleming, 1972, indicate an early to middle Miocene age.

Diatoms from a sample lower in the Cerro Tiza section (DV 591-1) include *Rouxia obesa* (H. Schrader, 28 January 1991, written communication), which had a first occurrence in foram Zone P18 (about 33.8 to 32 Ma; see Berggren et al., 1995). Superjacent channel-form glauconite and iron-manganese deposits with phosphatic nodules and rounded lithoclasts of dolomitzed sandstone (DV 483, 591, 2226) lie tens of meters below the Miocene unconformity.

Between Cerro Tiza and the Río Ica lies a depression (Samaca West) floored with coarse-grained bioclastic sandstone beds (DV 509, 544, 1812, 1901, 1902) that lap onto basement. Fossils in these beds (*Crassatella neorhynchus* Olsson, 1931, *T. lagunillasensis*) indicate an assignment to the Los Choros Member (DeVries, 2007, 2016). A measured section from basement to the first of three Otuma ashes (DV 1902, 1904) passes through the Yumaque/Otuma unconformity, which is defined by small cobbles of basement rock, lithoclasts, and nodules of iron and manganese (Figure 2D), stratigraphically several meters below a concretionary-weathering indurated white sandstone that had been incorrectly designated the base of the Otuma sequence (DeVries, 1998).

5.1.12. Samaca East

Sections of the Otuma sequence are exposed on the eastern side of the Río Ica in the Samaca area. A complete section (DV 7161, 7162; Figure 4D) was measured against eastern hills composed of crystalline basement rock, some of which stood above sea level as clustered Eocene sea stacks surrounded by oyster banks with barnacle and sea urchin debris (DV 7160). Two kilometers or less farther west, transgressive sandstone beds (DV 5082, 5083) with typical Otuma gastropods (*P. culberti*, *X. carditigera*), as well as oysters and sea urchins, overlie a black-pebble bed that separates the Otuma from the Paracas sequence, which also laps onto basement (DV 5080). (A second pebble bed, lower in the section and presumably within the Paracas Formation (DV 7165), bears further study.)

The basal coarse-grained, oyster-, barnacle-, and sea urchin-bearing Otuma sandstones in Samaca East are about 15 meters thick. They, in turn, are overlain with 20 meters of fining up medium- to fine-grained sandstone with an increasing silt component and a diverse assemblage of fish scales, including scales of clupeoids. The measured section at locality DV 7162 includes an additional 90 meters of fine-grained, soft-weathering sandstone with fish scales, interrupted at irregular intervals by indurated medium beds of medium-grained gray sandstone and indurated thin beds of dolomitized orange sandstone with fish scales. The stratigraphic succession of indurated orange dolomitic beds is repeated two kilometers to the west (DV 1716, 1727) and across the Río Ica at Samaca West (DV 546, 1813). An ash bed above the uppermost prominent orange dolomite horizon has an ^{40}Ar-^{39}Ar age of 35.7 Ma (DeVries, 1998). The sections on both sides of the Río Ica are truncated and in angular unconformity with overlying transgressive sandstone of the Chilcatay depositional sequence.

The distinctive orange dolomite beds of the Otuma sequence can be traced as southwest-dipping stripes on the eastern slopes of the Río Ica for ten kilometers south of Samaca (DV 1616, 1618, 1619, 4022), at which point poor exposures make it unclear whether the orange beds lie in fault contact or pass over crystalline basement rock.

5.1.13. Río Grande Valley and Quebrada Huaricangana

The Otuma sequence has yet to be identified in the valley of the Río Grande. Los Choros and Yumaque beds are well developed near Puerto Caballas (Dunbar et al., 1990), as are lower Eocene deposits of the Caballas depositional sequence (DeVries, in press). Undifferentiated Eocene deposits are exposed below lower upper Miocene tuffaceous sandstones of the Pisco Formation along the eastern and southern flanks of Cerro Terrestral (80JM 014, 83JM 021, DV 1456, 1965). An outcrop of orange sandstone overlying flinty fine-grained deposits at the landward edge of the 400-m Pleistocene terrace east of Quebrada Santa Cruz (DV 1457) might represent the base of the Otuma sequence. The best evidence for Otuma sediments on the east side of the Rio Grande is a collection of diatoms from locality 86JM 023 in Quebrada Huaricangana, with the same early Oligocene species, *Rouxia obesa*, as found at locality 86JM 060 (see above), near Salinas de Otuma (Macharé and Fourtanier, 1987) and DV 591-1, at Cerro Tiza.

5.2. Mid-Otuma Shoaling Event

The top of the type section of the Otuma Formation (DV 936) includes a fault-truncated exposure of black sandstone, several meters thick, composed of angular granules of granite. The gritty sandstone, which includes a small percentage of comminuted barnacles, oysters, and sea urchin spines, is separated by a scalloped erosive contact from an underlying coarse-grained orange sandstone with *Gyrolithes* burrows. The orange sandstone gradationally overlies silty sandstone with forams and clupeoid fish scales. The sequence of lithologies and trace fossils suggests a shoaling event. (See Dworschak and Rodrigues (1997) for a discussion of *Gyrolithes*).

Gritty black granitic sandstones are not confined to the Otuma type section. Southeast of Cerro Sombrero, a coarse-grained black sandstone bed occurs sandwiched between silty sandstones (DV 1222a, 3017; Figures 5A, 5B). A black-pebble sandstone also occurs mid-section in the Otuma sequence near the Carhuas-Comotrana Road (DV 631). On northern slopes of the downthrown block near Bajada del Diablo (DV 3026a) and along the route of Camino de los Burros (DV 3030), five meters of very poorly sorted and very coarse-grained sandstone and black-pebble conglomerate are overlain and underlain by more than forty meters of Otuma silty sandstone with pelagic microfossils and fish scales (Figures 5C, 5D). The erosive surface beneath the pebbly beds is scalloped with grooves oriented north-south. The topmost pebbly interval contains fragments of oyster valves. Broken oyster valves are also associated with a pebbly gravel in the lower mid-section of the Otuma section on Pampa Concha Roja (DV 5084).

Mid-Otuma shoaling is indicated at some localities not by granular black sandstone, but glauconitic sandstone, in some cases with phosphate nodules. The glauconite-phosphorite association in the modern Peruvian upwelling zone has been documented by Burnett (1980), Glenn et al. (1994), and Suits and Arthur (2000), who have discovered winnowed glauconite sands at upper to mid-slope depths, distributed along the lower margin of an oxygen minimum zone beneath areas of coastal upwelling.

At Quebrada Perdida (DV 3089, 3090, 3093), distinctive white-weathering, diatomaceous, *Coscinodiscus*-bearing silty sandstone of the lower half of the Otuma sequence is overlain by two meters of a massive, very coarse-grained, pebbly sandstone, largely glauconitic at its base (Figures 5E, 5F) and increasingly bioclastic near its top, with comminuted barnacles and fragments of oyster valves. A six-meter-thick interval of soft-weathering finer-grained sandstone separates the lower bioclastic glauconitic sandstone from a similarly coarse-grained upper sandstone that lacks barnacle fragments but does contain rip-up clasts of dolomitized silty sandstone. The second coarse-grained sandstone is overlain by 25 meters of finer-grained sandstone, which is capped by basal cobbly and lithoclast-bearing sandstone beds of the Chilcatay sequence.

Glauconite occurs at a similar stratigraphic position, also with thick sections of silty or fine-grained sandstone above and below, at Cerro Tiza (DV 591, 2226), but in a 20-meter wide channel-form deposit with associated iron and manganese concretions or nodules. On the northern edge of Pampa Negra, a 20-cm bed of glauconite with phosphate nodules (DV 7141) is overlain by several tens of meters of alternating fine-grained sandstone and bioturbated mudstone with burrows filled with glauconitic sand; the only fossils are poorly preserved forams.

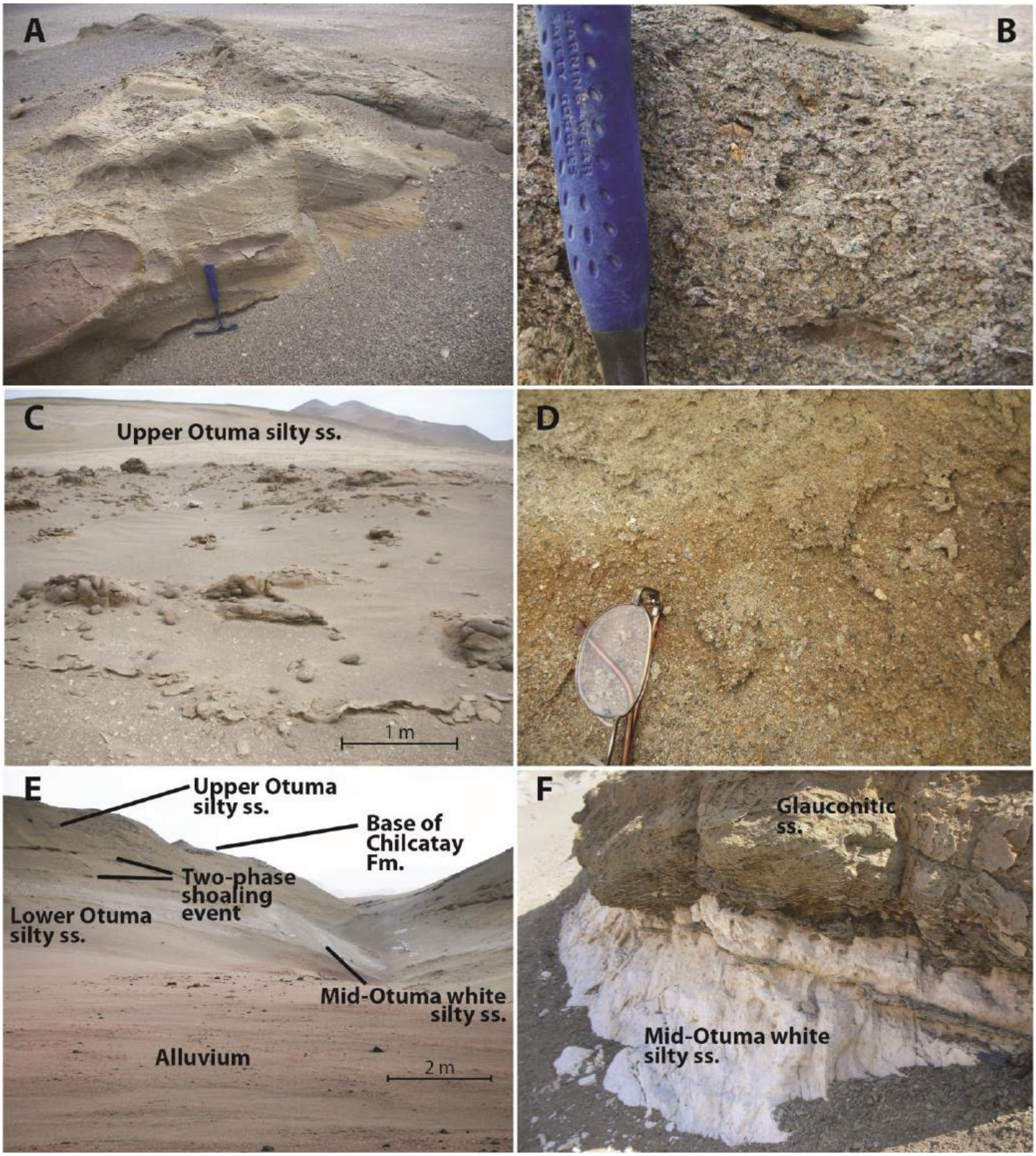

Figure 5. *Deposits indicating a mid-Otuma shoaling event. A, B. Crossbedded black-pebbly sandstone near Cerro Sombrero at DV 1222a and DV 3017. C, D. Black-pebbly sandstone along the Camino de los Burros at DV 3030. E. View northward into canyon emptying into Quebrada Perdida (DV 3089 and DV 3090) showing two indurated horizons between thick intervals of silty sandstone of the Otuma sequence. The two horizons may represent two episodes of rapidly falling sea level during the Eocene-Oligocene Transition. F. Glauconitic sandstone overlying silty sandstone with pelagic microfossils in Quebrada Perdida at DV 3093.*

5.3. Faunal Lists

5.3.1. Marine Mollusks

A list of marine mollusks found in the Otuma Formation was published in abstract form by DeVries (2004). An updated list is presented in Table I. A number of species from the Paracas Formation are included, as are a few Otuma species endemic to the East Pisco Basin to help identify Paracas and Otuma faunas in the field. Most of the listed species occur in both the Talara and East Pisco basins.

Table I. Selected fossil marine mollusks from the Pisco and Talara basins. Sources include Olsson (1928, 1930, 1931), Rivera (1957), and DeVries (1998, 2004).

SPECIES	PARACAS	OTUMA	OTUMA	OTUMA	TALARA BASIN		
	Prieto, Arquillo, Lagunillas	Talpo, Paracas neck	Santa Cruz, Playa Yumaque	Bajada del Diablo/ "Concha Roja"	Pre Chira/ Verdun	Chira-Verdun	Post Chira/ Verdun
Turritella lagunillasensis Rivera, 1957	x						
Cristispira paracasensis (Rivera, 1957)	x				x		
Epitonium peruvianum Olsson, 1928	x				x	x	
Dorsanum lagunitensis (Woods, 1922)	x				x	x	
Sulcobuccinum coronaria (Olsson, 1930)	x				x	x	
Sulcobuccinum monilis (Olsson, 1928)	x				x		
Andicula occidentalis (Woods, 1922)	x				x		
Xancus paytensis Olsson, 1928	x				x		
Olivancellaria inca Olsson, 1930	x				x	x	
Amotapus arbolensis (Woods, 1922)	x		x		x	x	
Sulcobuccinum parinasensis (Woods, 1922)	x	x		x	x	x	x
Xenophora carditigera Nielsen & DeVries, 2002	x?	x		x			
Melongena levifusoides Olsson, 1928				x	x	x	
Bursa chira Olsson, 1930				x	x	x	
Miltha woodi Olsson, 1930				x	x	x	x
Peruchilus culberti Olsson, 1931		x	x	x		x	x
Turritella cochleiformis (Gabb, 1869)			x	x		x	
Turritella woodsi Lisson, 1925		x	x	x		x	x
Ficus chiraensis Olsson, 1931			x	x		x	
Ectinochilus sp.			x	x		x	`
Morum charanalense Olsson, 1931				x			x
Voluta mancorensis Olsson, 1928				x		x	x
Architectonica sullana Olsson, 1928				x		x	
Architectonica chiraensis Olsson, 1928				x		x	
Tritaria sullana Olsson, 1931				x		x	
Turricula piura Olsson, 1931				x		x	
Clathrodrillia mira Olsson, 1931		x		x		x	
Cardita newelli Rivera, 1957		x	x	x			
Crassatella rafaeli DeVries, 2016				x			
"Dosinia" lechuzaensis Rivera, 1957		x	x	x			

The occurrence of several Otuma species in the Chira-Verdun sequence in the Talara Basin, first noted by Rivera (1957), supports a late Eocene age for the transgressive sandstone of the Otuma depositional sequence. Most Otuma species also occur in the sequence's uppermost fossiliferous beds on the Pampa Concha Roja (e.g., localities DV 4042, 4066, 5100), i.e., beds with a probable early Oligocene age.

5.3.2. Vertebrates

Notable among vertebrates found in the Otuma depositional sequence are several penguin species, including three described species: *Icadyptes salasi* Clarke et al., 2007; *Perudyptes devriesi* Clarke et al., 2007; and *Inkayacu paracasensis* Clarke et al., 2010 (Clarke et al., 2007, 2010; Ksepka, and Clarke, 2010), all three of which were found in transgressive sandstone or sediments transitional between the basal sandstone and overlying deeper-water silty sandstone

Owing to a miscommunication among field researchers, fossils of *P. devriesi* at Quebrada Perdida may have been attributed mistakenly to the Los Choros Member of the Paracas Formation (Clarke et al., 2007). During a later field season, the stratigraphic position of *Perudyptes* was re-evaluated: bones of *P. devriesi* might have been collected from the transgressive sandstones (DV 3059) of the Otuma Formation, overlying by decimeters the silty sandstone of the Yumaque Member and just 300 meters distant from a penguin bone-bearing sandstone of the Los Choros Member (DV 3060) and 100 meters distant from a partial penguin skeleton found in the Yumaque Member (DV 3063). Assuming a rapid Otuma transgression across the Peruvian coastal plain, the bones of *P. devriesi* would have an age of about 37-38 Ma based on ash dates in Samaca West (see above). Statements related to the paleogeographic setting for unnamed Los Choros and Yumaque penguins at Quebrada Perdida (Clarke et al., 2007) remain valid, including the assertion that the Los Choros and Yumaque bones represent the oldest known penguins from tropical latitudes.

The other fossil birds found in Otuma sediments are albatross-like pelagornithids. Pelagornithid bones from Playa Yumaque Southeast are housed in Lima at the Museo de Historia Natural, Universidad Nacional Mayor de San Marcos. Similar bones from Cerro Santa Cruz are at the Museo de Paleontología, Universidad de Ricardo Palma, also in Lima.

Of the several archeocete taxa found in the Otuma sequence, most undescribed, the basilosaurid, *Cynthiacetus peruvianus* Martinez and Muizon, 2011, is the most common. Disarticulated and partially articulated skeletal remains have been found near the base (Samaca East) and middle and top of the section (Pampa Concha Roja); along the entire north-south length of Otuma outcrop; and in transgressive sandstone, transitional nearshore/outer shelf sandstone, deeper-water silty sandstone, and the peculiar *Cardita*-rich shallow-water sandstone of Pampa Concha Roja.

Ten shark taxa have been identified in the Otuma Formation by A. Altamirano (Altamirano-Sierra, 2012; Altamirano-Sierra et al., 2011; also Altamirano-Sierra, 13 April 2016, written communication): *Carcharocles angustidens*, *Isurus* sp., *Striatolamia* sp., *Abdounia* sp., *Alopias* sp., *Carcharhinus* sp., *Carcharias* sp., *Sphyrna* sp., *Negaprion* sp., and *Odontaspis* sp. Bony fish found in Otuma sediments include clupeoids, represented by their scales, and unidentified billfish.

Crocodiles in the Otuma formation are represented by a new gavialoid taxon, possibly adapted to a coastal marine environment, found at Cerro Santa Cruz. Phylogenetic relationships of this long-snouted crocodile with Neogene gavialoids of South America are uncertain (R. Salas-Gismondi, 12 May 2016, written communication).

5.3.3. Wood

Fossil wood is encountered in nearshore marine sandstone of the Paracas, Otuma, Chilcatay, and Pisco sequences, as well as in alluvial sandstone of the lower Eocene Caballas sequence. To date, not one study of Cenozoic plants from the East Pisco Basin has been undertaken. Thus, this report constitutes the first published account of fossil wood from this basin.

Wood occurs throughout the Otuma sequence, but is most often found on the Pampa Concha Roja in the lower section (DV 5084, 7119) in soft-weathering sandstone that also contains dispersed valves of *Cardita newelli* and small venerids, and in the upper part of the section (DV 7092, 7102), where large tree trunks are interspersed with lenses of mudstone, pumice-laden, ashy, *Ophiomorpha*-burrowed sandstone (Figure 6A), and mollusk-bearing bioclastic sandstone (Figure 6B). In much of the section, as is the case for most of the East Pisco Basin, the wood is imperfectly replaced with a mixture of iron, manganese, and gypsum. The tree trunks at the top of the Otuma sequence, however, are silicified and therefore subject to traditional sectioning analysis.

At locality DV 5087, a tree trunk with a diameter of 70 cm is embedded at a 45-degree angle in a sandstone bed (Figure 6C). Allometric scaling relationships for tropical trees allow us to estimate tree height of ~33 meters based on 70 cm diameter at breast height (Rich et al. 1986; Feldpausch et al. 2011). In size and texture, the tree trunk is identical with others a few meters higher in the section, all of which came to rest horizontally (Figure 6D) and some of which were bored by marine bivalves.

The angled tree trunk has been identified by one of the authors (N. A. Jud) as a probable member of the legume family, Fabaceae Lindley, 1836, subfamily Caesalpinioideae Linné, 1753, based on the presence of simple perforation plates, similar intervessel and vessel-ray parenchyma pitting, storied structure, undulating bands of axial parenchyma, and uniformly biserate rays. The diffuse-porous wood lacking tree rings indicates the tree grew in a minimally seasonal tropical setting. The Otuma legume is similar to the "garapa," a wide-ranging, drought-tolerant, emergent or canopy tree of South American tropical forests that can grow to a height of 50 meters (de Portugal et al. 2010). The Otuma wood's estimated low density (Martinez-Carbrera et al. 2012) indicates the tree likely grew under bright conditions and had a ready source of water.

The Otuma tree is the first fossil occurrence of Fabaceae in Peru and only the third reported occurrence of a fossil legume in Peru (Pujana et al., 2011). A complete description of the wood will be presented in a later contribution.

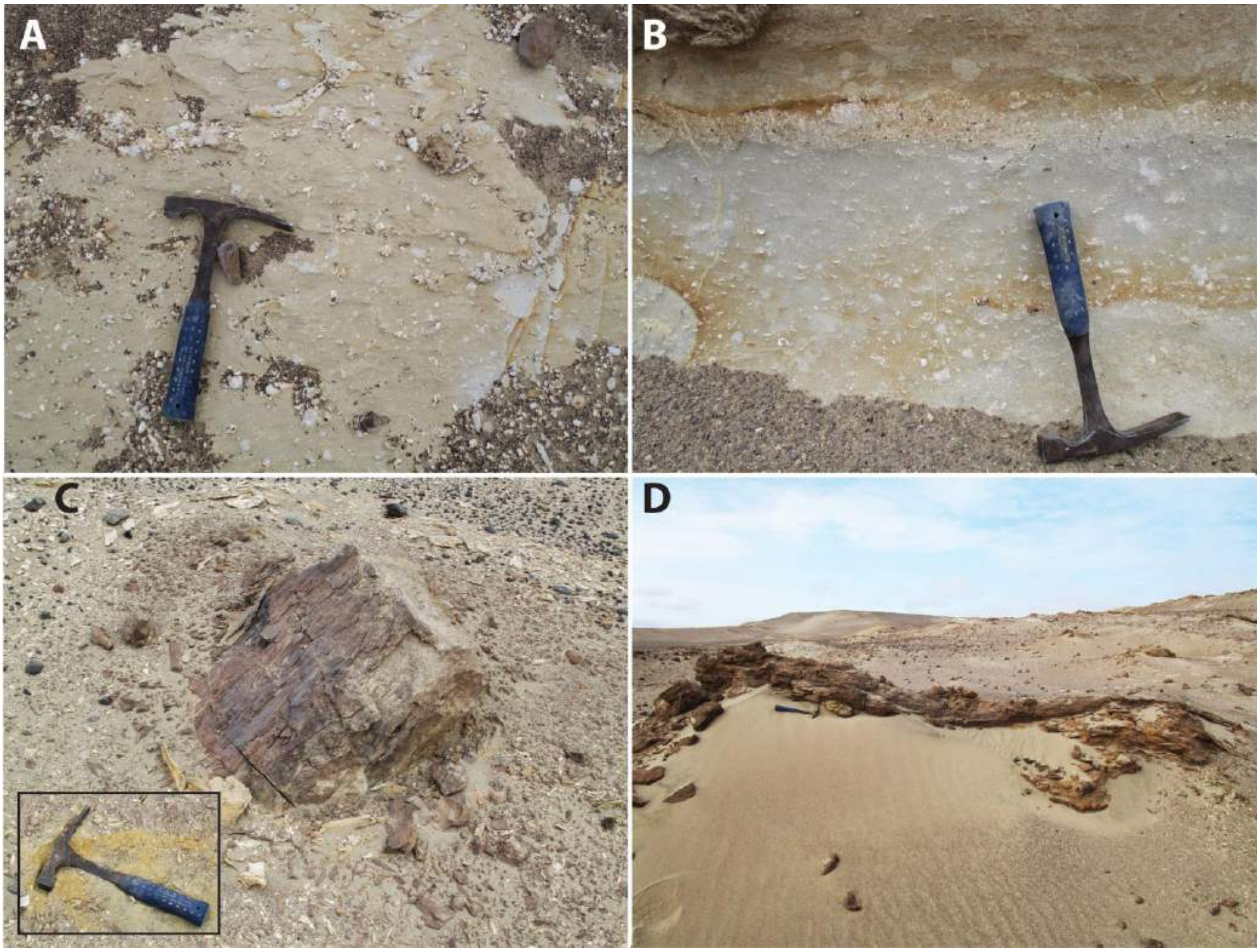

***Figure 6**. Fossil wood and lithofacies of Unit H of the Otuma sequence at Pampa Concha Roja. A. Ash-filled Ophiomorpha burrows at DV 5087. B. Shell lags of Cardita newelli and small venerids interbedded with bioturbated sandstone with dispersed valves of the same two species at DV 5089. C. Tilted trunk of legume tree embedded in former sandbar at DV 5087. D. Tree trunk lying horizontal in midst of bioclastic sandstone, ashy sandstone, and mudstone lenses at DV 5092.*

6. Discussion

6.1. Otuma Paleogeography

6.1.1. Comments on the Structural History of the Basin

To properly reconstruct the paleogeography of the East Pisco Pasin coast during the late Eocene and early Oligocene requires an appreciation of the basin's structural history. Since the late Pliocene, the basin has been uplifted by as little as 60 meters (DV 828) at its northern limit to more than 800 meters at its southern limit of Cerro Huaricangana (DV 484, 511), as measured by the elevation of marine terraces with a modern or late Pliocene molluscan fauna (DeVries, unpublished data; Macharé, 1987; Macharé and Ortleib, 1992) and extrapolated rates of uplift based on ^{10}Be dating of terrace surfaces near San Juan de Marcona (Saillard et al., 2011). More typical are post-Pliocene uplifts of 160 to 200 meters as demonstrated by relicts of marine terraces with late Pliocene mollusks 15 kilometers inside the Río Ica valley (DV 1028).

Comparable vertical offsets affecting blocks with upper Miocene strata (Figure 7) occurred along several major normal faults: the west-southwest dipping Monte Grande and Río Ica faults, with 200 meters of vertical throw; the north-dipping Ullujaya Fault and the south-southwest dipping footwalls of the Bajada el Diablo / Camino del Burro and Quebrada Perdida half-grabens, with 400+ meters of vertical throw; the southeast-dipping Great Sand Valley Fault, with 200 m of vertical throw that would have juxtaposed crystalline basement rock with eastward tilting beds of the Otuma Formation were it not for erosion of Otuma strata from the Great Sand Valley; and the north-northeast dipping Paracas and east-dipping Cerro Santa Cruz faults.

North-south extension associated with the east-west striking master faults of the half-grabens at Quebrada Perdida and Bajada del Diablo / Camino de los Burros and the Ullujaya Fault may be related to the southward longshore sweep of the obliquely subducting Nazca Ridge, which impinged on the South American plate at 11°S at about 11 Ma (Hampel, 2002) and currently intersects the Peruvian margin at about 15°S, where it extends beneath Cerro Huaricangana. East-west extension, a stress pattern evidenced throughout the East Pisco Basin by the prevalent north-south strike of mid-sized normal faults (Figure 7), has affected Neogene strata but also had occurred prior to

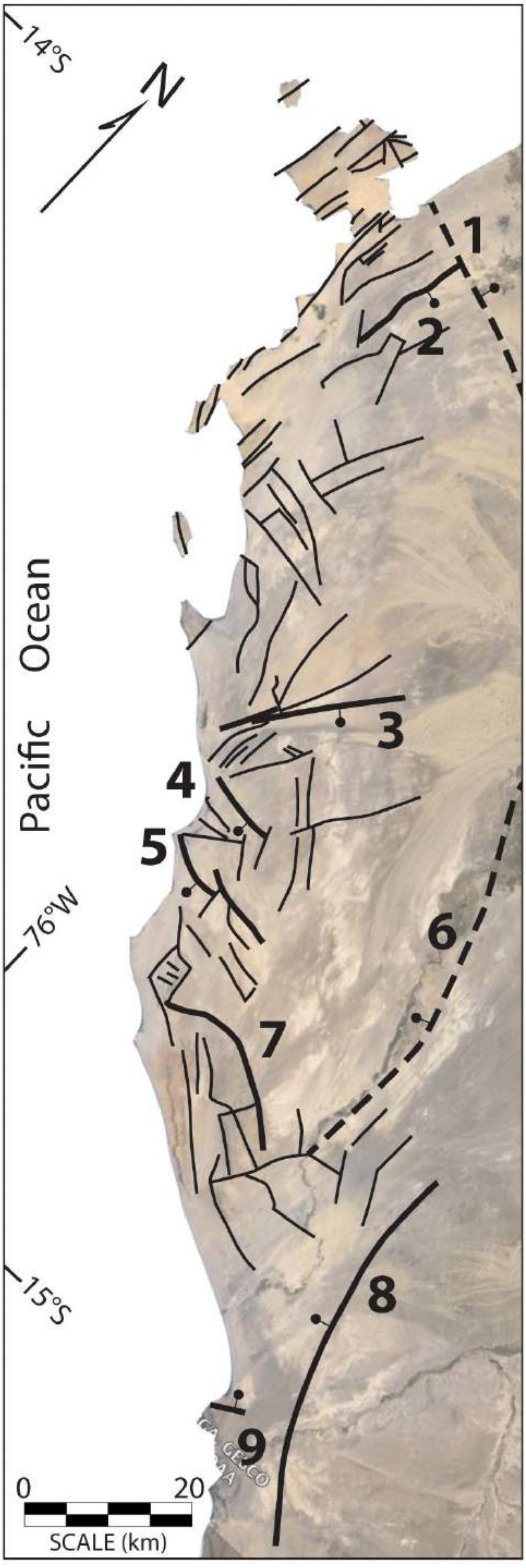

Figure 7. Fault patterns in the East Pisco Basin. A fabric of north-south striking mid-sized normal faults prevails throughout the basin but is more pronounced around the Paracas Peninsula. It is unclear if the mid-sized faults and the two major north-northwest normal faults in the central and southern East Pisco Basin share a common origin. A major east-west striking fault defines the northern exposure of basement and Paleogene outcrop at the latitude of Paracas. Other east-west lineations are the master faults of half-grabens. Numbered features: 1. Paracas Fault. 2. Cerro Santa Cruz Fault. 3. Great Sand Valley Fault. 4. Bajada del Diablo / Camino de los Burros Master Fault. 5. Quebrada Perdida Master Fault. 6. Río Ica Fault. 7. Ullujaya Fault. 8. Monte Grande Fault. 9. Caballas Master Fault.

the latest Oligocene, judging from the effect on patterns of basal bioclastic sandstone onlapping mid-sized (2 to 10 kilometers long) faulted blocks of crystalline basement rock and the failure of many faults to extend through the angular unconformity marking the onset of Chilcatay deposition. The pattern of multidirectional sediment sources for onlapping basal Otuma sandstone indicates that east-west extension also created a complex late Eocene, pre-Otuma basement topography, particularly in the areas of the Paracas Peninsula and Río Ica.

6.1.2. Paleogeographic Regions

Lithofacies of the Otuma depositional sequence vary according to such fundamentals as water depth, exposure to wave action, and sediment source, all of which relate to the contour and topography of the Otuma coastline. Ages of microfossils from the Paracas sequence and ash beds from the Otuma sequence show that a late Eocene coastal plain, which was undergirded by crystalline basement rock and Paracas sediments, had been emergent for two million years prior to the Otuma transgression.

The easternmost extent of Otuma outcrop (Figure 8) coincides with the easternmost extent of the basal transgressive sandstone. At some latitudes, the presence of crystalline basement boulders in basal beds or influxes of pebbly sandstone in the mid-Otuma section indicates the point of maximum transgression and a rugged coastal plain might not be much farther to the east. At other latitudes, thick sections of silty sandstone with pelagic microfossils at the easternmost limit of outcrop indicate that the Otuma shoreline could have been located much farther eastward. Such might not be the case, however: 'deep-water' sediments can be deposited surprisingly close to shore. Diatomaeous silty sandstone was deposited less than two kilometers offshore from shoreface boulder conglomerates in the late Miocene Nazca embayment (DeVries, 1988) and modern marine diatomaceous muds accumulate at water depths as little as one meter in Walvis Bay, Namibia (Bremner, 1980).

An Otuma shoreline that probably marks an intermediate stage of transgression (Figure 8) features four distinct segments. To the north, the "Paracas Archipelago" consisted of small islands of crystalline basement rock, shedding sediments to the east and west during early Otuma time into shallow, sandy, protected passages; and a mainland shoreline studded with granitic sea stacks and aprons of bioclastic debris. South of the archipelago, the "Quemado Peninsula" jutted westward from Ica. The former peninsula today forms an elevated pampa, with no evidence of early Cenozoic sediments across its desolate expanse except for downthrown blocks near Morro Quemado (DV 1135) and alongside the Great Sand Valley (DV 2247). The only sedimentary rocks that do overlie the modern Quemado pampa are Miocene sandstones of the Pisco Formation, which are thickest in one arc that crosses the Carhuas-Comotrana Road (DV 5002) and a second arc to the south (DV 1134), but do appear, too, in isolated outcrops on the southeastern side of the pampa (DV 3036).

The largest segment of the Otuma coast, herein termed the "Ullujaya Margin," extends southward from the Great Sand Valley for 100 kilometers before disappearing in the basement outcrops of Cerro Huaricangana and pockets of Eocene sediment surrounding San Juan de Marcona. At the northern limit of the Ullujaya Margin lay a broad indentation in the coastline termed "Bahía Concha Roja."

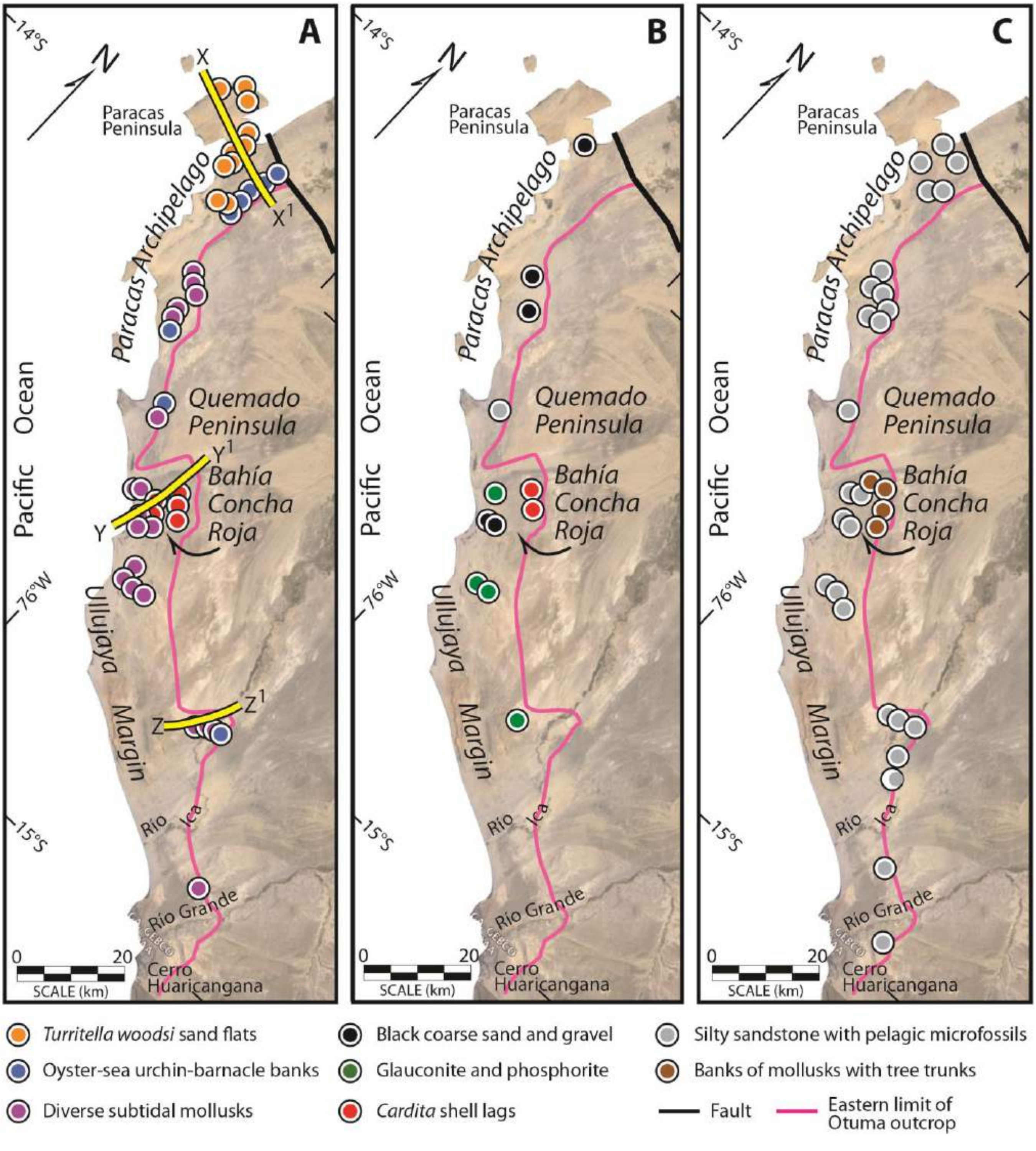

Figure 8. *Paleogeographic reconstruction of the East Pisco Basin and distribution of lithofacies. A. Early phase of Otuma deposition. B. Eocene-Oligocene Transition (EOT) phase. C. Late phase of Otuma deposition. The northern limit of Eocene-Oligocene outcrop is defined by an east-west fault near the Paracas Peninsula. The marked eastern edge of Otuma outcrop probably follows the Otuma shoreline at early and mid-transgressive phases. The maximum extent of transgression is obscured by Neogene and Quaternary deposits or removed by erosion but may not extend much farther inland (see text).*

6.1.3. The Paracas Archipelago

Outcrops of the Eocene Paracas Archipelago are truncated at the latitude of Paracas by the east-west striking Paracas Fault that juxtaposes late Neogene sediments of the Pisco Formation to the north with basement rocks, Eocene marine sediments, and early Miocene deposits of the Chilcatay Formation. To the south, the Paracas Archipelago ends at the Quemado Peninsula.

Transgressive Otuma sandstone beds that crop out from the Paracas Peninsula (87DV 502) to Playa Yumaque and Pampa Las Salinas contain dense accumulations of *Turritella woodsi*, often size-sorted, and lesser numbers of small oysters and venerid clams (Figures 8A, 9A). The gregarious habits adopted by some modern shallow-dwelling turritelline species are well documented (Allmon, 1988, 2011). The archipelagan geography would have created protected sand flats for masses of turritellines and small venerids. Oysters are inferred to have lived on the islands' rocky shores, since no oysters were found attached to other mollusks. Landward, turritellines became less numerous and oysters, sea urchins, and barnacles, more numerous, especially in the channels between paleo-sea stacks. The presence of primary gypsum and crinkled marls indicates that some archipelago inlets experienced very restricted circulation and intense evaporation. It is in this setting of shallow channels and evaporative lagoons that penguins, giant and otherwise (Clarke et al., 2007, 2010), made their home, as did pelagornithid birds, gavialoid crocodiles, sharks, and cheloniid sea turtles (Altamirano-Sierra et al., 2011).

Farther south, perhaps where there were fewer protective islands, transgressive sandstone beds contain a greater diversity of mollusks – the same cast of taxa (*Bursa, Peruchilus, T. woodsi*, *Xenophora*, *Cardita*, *Corbula*, venerids) that also occurs in medium-grained sandstone beds that overlie the turritelline beds farther north. It was during this later phase of transgression in the northern East Pisco Basin, in slightly deeper and probably more open waters, that the archeocete, *Cynthiacetus*, made its appearance (type locality: 13°52'54"S, 76°14'14"W; Martinez-Caceres and Muizon, 2011).

Overlying the mollusk-bearing sandstones of the Paracas Archipelago are the same Otuma silty sandstones with pelagic microfossils, clupeoid fish scales, and tiny thin-shelled pectinids seen throughout most of the East Pisco Basin (Figures 8C, 9A). During the mid-sequence shoaling event, the silty sandstones were scoured and overlain by gritty black pebbly sandstones derived from basement crystalline rock (Figure 8B), indicating that Otuma waters were shallower than the drop in sea level and/or that a steepened gradient of the nearby coast resulted in more vigorous erosion and offshore transport of weathered debris from exposed basement rock.

6.1.4. The Quemado Peninsula and Bahía Concha Roja

The Quemado Peninsula separated turritelline sand flats of the Paracas Archipelago from a *Cardita*-dominated assemblage in Bahía Concha Roja (Figures 8A, 9B). *Cardita newelli* is present in most Otuma transgressive sandstones, usually one of many equally common molluscan species in beds whose stratigraphic position between underlying oyster-bearing coarse-grained sandstone and overlying silty sandstone with pelagic microfossils indicates an inner shelf setting. However, on Pampa Concha Roja *Cardita* is often the dominant species and occurs throughout the section, either dispersed or concentrated in shell lags (Figures 6D, 8B, 8C, 9B). Modern carditids often live attached to rocky shorelines (e.g., Riascos et al., 2008), but a better ecological analog for the carditids of Bahía Concha Roja might be the association of modern *Cardita calyculata* (Linné, 1758) with sea grass meadows on the coast of Tunisia (Belgacem et al., 2014).

Some shell lags consist almost exclusively of *C. newelli*; others, small venerids; in rare cases, *T. woodsi*; and in a few beds, an equal mix of those three taxa and lesser numbers of *Bursa*, buccinids, *C. rafaeli*, *Corbula*, and large venerids, The most diverse shell lags and largest numbers of *T. woodsi* occur near the bottom and top of the sequence, i.e., the shallow waters of early transgressive and late-sequence prograding phases. Venerid-dominated shell lags are most common just higher in the section above the high-diversity shell lags. *Cardita*-dominated shell lags occur closer to the middle of the sequence, from both the top and bottom of the section. (The lower *Cardita*-dominated interval has a pebbly sandstone bed.) Poorly fossiliferous muddy sandstone with intercalated beds of afossiliferous indurated sandstone are prevalent in the middle of the section.

This sequence of molluscan assemblages and sediments in Bahía Concha Roja is interpreted to represent a steady deepening of Bahía Concha Roja, from open-marine high-energy subtidal environments (diverse mollusks, channels, cobbles), to less energetic environments (dispersed venerids in bioturbated sandstones and venerid shell lags), to subtidal sea grass meadows with dispersed and concentrated lags of *Cardita*, often nearly monospecific), to deeper-water mudstones, perhaps deposited in hypoxic conditions, with only small bivalves preserved (*Nucula*, tiny mactrids). The deepening was evidently interrupted by a period of high-energy deposition, perhaps shoaling, marked by the pebbly coarse-grained sandstone with fragments of bivalves. A later phase of shoaling coincided with prograding subtidal sands with sea-grass meadows, culminating with sand and mud flats so shallow that they could strand large trunks of the Eocene garapa tree. The tree-trunk-dotted sand flats crop out for a paleo-longshore distance of at least five kilometers. The large number of leguminous tree trunks points to a nearby source, perhaps a river alongside the south side of the Quemado Peninsula coinciding with the course of the Great Sand Valley.

The *Cardita*-dominated lithofacies of Bahía Concha Roja rapidly fades to the west. On Pampa Negra (DV 5109) and inside Bajada del Diablo (DV 1442, 1443, 1444, 3025, 3026, 3028, 3029), venerids and *Cardita* valves are restricted to the basal 40 meters of transgressive sandstone, which are overlain by silty sandstone with clupeoid scales and pelagic microfossils (Figures 8A, 8C, 9B). To the west and south of Pampa Negra, i.e., at passes overlooking Playa Palo Vento (DV 7142, 7144) and near the granitic footwall of the half-graben at Bajada del Diablo / Camino de los Burros (DV 5110, 5111, 5112), the Otuma basal transgressive sandstones have fewer venerid and *Cardita* bivalves and are increasingly conglomeratic, suggesting both a higher energy of deposition and a nearby source of large crystalline basement clasts – perhaps the Quemado Peninsula.

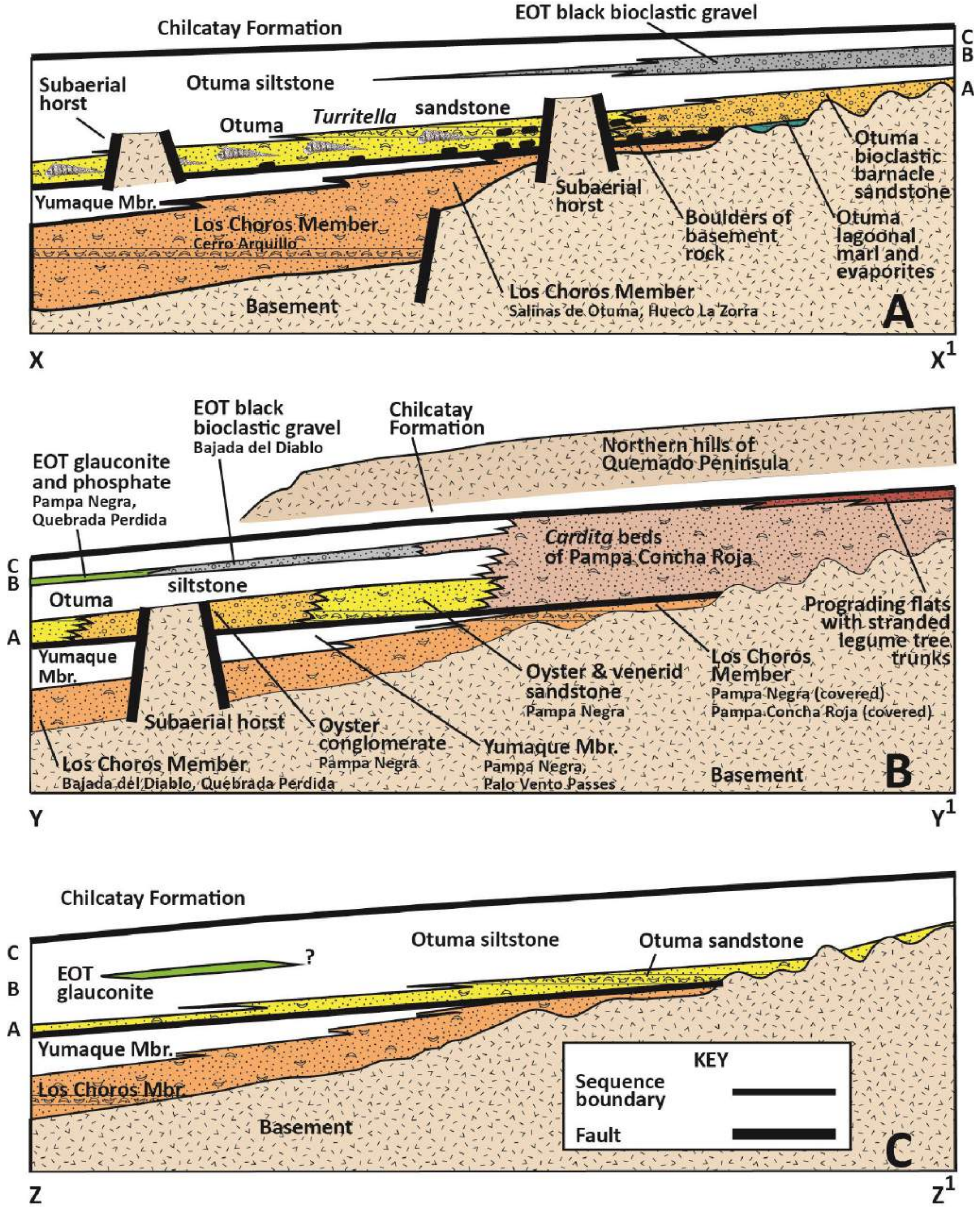

***Figure 9**. Schematic cross sections of the Paracas and Otuma sequences (see Figure 8A for profile locations). A. Paracas Archipelago, profile X-X1. B. Bahía Concha Roja, profile Y-Y1. C. Ullujaya Margin, profile Z-Z1. A horst (A) and the elevated Quemado Peninsula (B) that are not in the section but affected lithofacies development are shown as detached features. Faults and horsts are inferred from differential section thicknesses and lithofacies distribution. EOT = Eocene-Oligocene transtion (see text).*

6.1.5. Ullujaya Margin

From the Bajada del Diablo / Camino de los Burros half-graben southward along the Eocene Ullujaya Margin to Cerro Huaricangana, the Otuma depositional sequence shows a nearly uniform succession of lithofacies and faunas (Figures 8A, 8C, 9C). Basal transgressive shallow-water sandstone beds have a diverse assemblage of mollusks (*Bursa*, *Peruchilus*, *Xenophora*, *Cardita*, venerids). Deepening water is indicated by fining-up beds of sandstone transitioning to silty sandstone, decreasing numbers of mid-sized mollusks, increasing numbers of thin and millimeter-sized mollusks, and the appearance of clupeoid fish scales and pelagic microfossils – a succession, incidentally, that is repeated with different species in the Paracas, Chilcatay, and Pisco depositional sequences. The mid-sequence shoaling event is represented by glauconite, not black-pebble sandstone (Figures 8B, 9B). The silty sandstones are intercalated by indurated orange-brown beds of dolomitized sediment, geochemically also characteristic of the modern coastal upwelling zone off Peru (Suess et al., 1987).

Continental shelf waters off the Ullujaya Margin were occupied by the ubiquitous archeocete, *Cynthiacetus*, and several penguin species, including *Perudyptes devriesi*. The diversity and perhaps abundance of Otuma vertebrates was greatest at Samaca East, where partial skeletons have been found of *Cynthiacetus* and other basilosaurids; the giant penguin, *Icadyptes salasi*; and cheloniid sea turtles. The abundance and high diversity of fish scales in the Samaca East sandstone beds might indicate an elevated secondary productivity that could have supported apex predators.

6.2. Eocene-Oligocene Transition

The Eocene-Oligocene Transition (EOT) was a brief time when the global climate rapidly cooled and the Antarctic ice sheet rapidly grew (Coxall et al., 2005; Lear et al., 2008; Zachos et al., 2008). Two episodes of falling sea level have been associated with the ice sheet growth, one coinciding with the EOT-1 oxygen isotopic shift at about 33.8 Ma, the other coinciding with the Oi-1 isotopic shift at about 33.5 Ma (terminology after Miller et al., 2008; ages according to Coxall et al., 2005), with sea level drops estimated at 20 meters and 50-60 meters, respectively (Houben et al., 2012). It is plausible that one or both of these drops in eustatic sea level could have produced the lithologic shoaling signal seen in the middle to upper Otuma depositional sequence (Figure 9).

The timing of the EOT and associated episodes of falling sea level remains insufficiently constrained in the Otuma section of the East Pisco Basin. There is wealth of radiometric and microfossil data documenting the age of the Otuma depositional sequence below the shoaling horizons: ash beds as young as 35.7 Ma (DeVries et al., 2006), foraminifera from the mid-section of the Otuma sequence on the Pampa Las Salinas with an age between 35.5 and 34.4 Ma (Ibaraki, 1993), Eocene nannofossils from Cuenca Sombrero older than 36 Ma (DeVries et al., 2006), and radiolarians at Quebrada Perdida with ages 36.3 to 33.6 Ma (DeVries et al., 2006).

Evidence for ages younger than the EOT sea level events is less compelling, largely because so few samples have been analyzed from the several tens of meters of silty sandstone that overlie the beds of black-pebble or glauconitic sandstone. The early Oligocene diatom, *Rouxia obesa*, occurs in samples of silty sandstone from Pampa Las Salinas (Macharé and Fourtanier, 1987), Cerro Tiza, and Quebrada Huaricangana. Foraminifera from Playa Supay, south of Playa Yumaque (Ibaraki, 1993), indicate an age of 33.7 to 32 Ma (Berggren and Pearson, 2005). Diatoms from the Carhuas-Comotrana Road point to Otuma ages between 35 and 33 Ma.

Pending a more systematic approach to microfossil sampling, stratigraphic and microfossil evidence to date indicates that the Otuma depositional sequence spans the latest Eocene to early Oligocene and likely includes a record of the EOT.

7. Conclusions

This paper describes a thirty-year-long field reconnaissance of the East Pisco Basin. As such, it only scratches the surface of what more can be learned between Pisco and Nazca – stratigraphically, lithologically, paleontologically.

The Otuma transgression commenced between 37 and 38 Ma. The degree of the transgression's diachroneity from one outcrop to the next across the basin is unknown. Broad patterns of lithofacies have been identified and used in conjunction with the distribution of crystalline basement outcrop and paleoecological data to reconstruct the late Eocene and early Oligocene paleogeography of the East Pisco Basin. Four distinct costal zones have been identified – a northern archipelago, a central peninsula, a tree-lined embayment south of the peninsula, and a long open shoreline to the south. These four zones had a history of deposition slightly or greatly different than one another and supported invertebrate and vertebrate faunas that also differed depending on time and place in the East Pisco Basin.

More stratigraphic and sedimentological fieldwork remains: matching patterns of clast petrology and clast diameter with maps of basement outcrop; measuring more sections at a finer scale; and carefully stitching together overlapping stratigraphic sections from Pampa Concha Roja. New areas of outcrop remain to be visited or revisited: outcrops between Morro Quemado and the Great Sand Valley, the lower reaches of the Río Ica valley, and Quebrada Huaricangana.

A systematic approach to building a chronostratigraphic framework for the Otuma sequence (not to mention the entire Cenozoic section of the East Pisco Basin) has yet to be undertaken. Sampling at regular intervals for diatoms, foraminifera, radiolarians, and nannofossils would complement radiometric data and help constrain the age range of the Otuma sequence, as well as the age of the Eocene-Oligocene Transition that is probably represented lithologically in the Otuma sequence. Evidence of the EOT in the Otuma sequence was stumbled upon; a concerted effort to find more outcrops with evidence of shoaling events and to characterize them more completely in terms of lithology, sedimentary structures, and chemistry and to combine that data with paleoceanographic insights provided by microfossil assemblages above and below the shoaling event might shed light on the interplay between global ocean circulation patterns and coastal upwelling.

A better understanding of basinal marine paleoecology might be obtained by quantifying the relative abundances of molluscan taxa in the transgressive sandstone and integrating invertebrate with vertebrate data. Onshore, the only window on the Eocene ecology of the coastal plain is provided by the abundant floral remains in marine sediments. More woody taxa are preserved in Otuma beds than the single garapa-like tree introduced in this paper. The extent to which pollen are preserved in Otuma sediments has never been determined.

To conclude, three broad directives for future investigation are proposed.

1. Characterize the world's archetypal coastal upwelling ecosystem as it evolved through the EOT, focusing primarily on the microfossil and lithostratigraphic record but also taking into account the invertebrate and vertebrate faunas, especially penguins and archeocetes.

2. Explore the possibility of a comprehensive palynological record in the Otuma section and systematically collect and identify woody debris found throughout the section, even material preserved as manganese-iron-gypsiferous crusts.

3. Consider the paleogeographic and paleoceanographic role that the West Pisco Basin, now submergent (Azalgara, 1994), might have played in the development of late Eocene and early Oligocene lithofacies, faunas, and floras in the East Pisco Basin.

Acknowledgements

Assistance was provided with either vertebrate species lists, microfossil identification, lithostratigraphic and biostratigraphic zonal nomenclature, radiometric data, or translation by Ali Altamirano-Sierra, Aldo Benites Palomino, Rodolfo Salas-Gismondi, and Marcelo Stucchi, all presently or formerly associated with the Departamento de Paleontología de Vertebrados, Museo de Historia Natural Javier Prado, Universidad Nacional Mayor de San Marcos (Lima, Peru), Patrice Baby (Institut de Recherche pour le Développement (IRD), Marseilles, France), Sebastien Carretier (IRD, Santiago, Chile), César Chacaltana (Instituto Geológico Minero y Metalúrgico, Lima, Peru), Brian Huber (Department of Paleobiology, Smithsonian National Museum of Natural History, Washington, D.C., USA), José Macharé Ordoñez (Instituto Geofísico del Perú, Lima, Peru), Kevin Nick (Department of Earth and Biological Sciences, Loma Linda University, Loma Linda, California, USA), Elisa Malinverno (Dipartimento di Scienze dell'Ambiente e del Territorio e di Scienze della Terra, Università degli Studi di Milano-Bicocca, Milan, Italy), and during the 1980s and 1990s, Hans Schrader (Institutt for Geovitenskap, Universitetet i Bergen, Bergen, Norway), John Barron (United States Geological Survey (USGS), Menlo Park, California, and Larry Snee (USGS, Denver, Colorado). Helpful critiques of the manuscript were provided by Alfredo Pardo A. (Graña y Montero Petrolera, Lima, Peru) and René Marocco (IRD, Montpellier, France). Rafael Casas (Ica, Peru) has acted as driver and field guide for several field seasons. Field work was in part funded by the Granville Research Institute (Granville, Ohio USA).

References

Allmon, W.D. 1988. Ecology of Recent turritelline gastropods (Prosobranchia, Turritellidae): Current knowledge and paleontological implications. Palaios, v. 3, p. 259-284.

Allmon, W.D. 2011. Natural history of turritelline gastropods (Cerithiodea: Turritellidae): A status report. Malacologia, v. 54, p. 159-202.

Altamirano-Sierra, A. 2012. Toward a review of sharks (Chondrichthyes: Selachii) of Peru: Past and present. III Encuentro Colombiano sobre Condrictios, Santa Marta, Colombia, 29 October - 2 November, 2012. Unpaginated.

Altamirano-Sierra, A., DeVries, T., Salas-Gismondi, R., Urbina, M., Ksepka, D., Clarke, J.A. 2011. Sphenisciform remains and other fossil vertebrates from the Otuma formation in the Paracas National Reserve, Peru. Ameghiniana, v. 48, p. R136.

Azalgara, C. 1994. Structural evolution of the offshore forearc basins of Peru, including the Salaverry, Trujillo, Lima, West Pisco and East Pisco Basins. Masters thesis, Rice University, Houston, Texas, USA, 178 p.

Baldauf, J.G. 1992. Middle Eocene through early Miocene diatom floral turnover. *In*: Eocene-Oligocene climatic and biotic evolution, Prothero, D.R., Berggren, W.A. (eds.), Princeton University Press, Princeton, New Jersey, USA, p. 310-326.

Baldauf, J.G., Barron, J.A. 1991. Diatom biostratigraphy: Kerguelen Plateau and Prydz Bay regions of the Southern Ocean. In: Proceedings of the Ocean Drilling Program, Scientific Results, Barron, J.A., Larsen, B., et al., Ocean Drilling Program, College Station, Texas, USA, v. 119, p. 547-598.

Belgacem, W., Langar, H., Pergent, G., Kalthoum Ben Hassine, O. 2013. Associated mollusc communities of a *Posidonia oceanica* meadow in Cap Zebib (off North East Tunisia). Aquatic Botany, v. 104, p. 170-175.

Berggren, W.A., Kent, D.V., Swisher, III, C.W., Aubry, M.-P. 1995. A revised Cenozoic geochronology and chronostratigraphy. SEPM Special Publication, v. 54, p. 129-212.

Berggren, W.A., Miller, K.G. 1988. Paleogene tropical planktonic foraminiferal biostratigraphy and magnetobiochronology. Micropaleontology, v. 34, p. 362-380.

Berggren, W.A., Pearson, P.N. 2005. A revised tropical to subtropical Paleogene planktonic foraminiferal zonation. Journal of Foraminiferal Research, v. 35, p. 279-298.

Blow, W.H. 1969. Late middle Eocene to Recent planktonic foraminiferal biostratigraphy. *In*: Proceedings of the First International Conference on Planktonic Microfossils (Geneva, Switzerland, 1967), Bronnimann, P., Renz, H.H. (eds.), E.J. Brill, Leiden, The Netherlands, v. 1, p. 199-421.

Bolli, H.M., Saunders, J.B. 1985. Oligocene to Holocene low latitude planktic foraminifera. *In*: Plankton Stratigraphy, Bolli, H.M., Saunders, J.B., Perch-Nilsen, K. (eds.), Cambridge University Press, Cambridge, England, p. 155-262.

Bremner, J.M. 1980. Physical parameters of the diatomaceous mud belt off South West Africa. Marine Geology, v. 34, p. M67-M76.

Burnett, W.C. 1980. Apatite-glauconite associations off Peru and Chile: palaeo-oceanographic implications. Journal of the Geological Society of London, v. 137, p. 757-764.

Catuneanu, O., Galloway, W.E., Kendall, C.G. St. C., Miall, A.D., Posamentier, H.W., Strasser, A., Tucker, M.E. 2011. Sequence stratigraphy: Methodology and nomenclature. Newsletters on Stratigraphy, v. 44, p. 173-245.

Clarke, J.A., Ksepka, D.T., Salas-Gismondi, R., Altamirano, A.J., Shawkey, M.D., D'Alba, L., Vinther, J., DeVries, T.J., Baby, P. 2010. Fossil evidence for evolution of the shape and color of penguin feathers. Science, v. 330, p. 954-957.

Clarke, J.A., Ksepka, D.T., Stucchi, M., Urbina, M., Giannini, N., Bertelli, S., Narváez, Y., Boyd, C.A. 2007. Paleogene equatorial penguins challenge the proposed relationship between biogeography, diversity, and Cenozoic climate change. Proceedings of the National Academy of Sciences, v. 104, p. 11545-11550.

Coxall, H.K., Wilson, P.A., Pälike, H., Lear, C.H., Backman, J. 2005. Rapid stepwise onset of Antarctic glaciation and deeper calcite compensation in the Pacific Ocean. Nature, v. 433, p. 53-57.

DeVries, T.J. 1988. Paleoenvironments of the Pisco Basin. *In*: Cenozoic geology of the Pisco Basin. A guidebook to accompany a regional IGCP 156 field workshop: "Genesis of Cenozoic phosphorites and associated organic-rich sediments: Peruvian continental margin" (May 16-25, 1988), Dunbar, R.B., Baker, P.A. (eds.), p. 41-49.

DeVries, T.J. 1998. Oligocene deposition and Cenozoic sequence boundaries in the Pisco Basin (Peru). Journal of South American Earth Sciences, v. 11, p. 217-231.

DeVries, T.J. 2004. Eocene mollusks from the Pisco Basin (southern Peru): Evidence for re-evaluating the age of the Otuma Formation. XII Congreso Peruano de Geología, Lima, Peru, October, 2004. Sociedad Geológica del Perú, Resúmenes Extendidos, Publicación Especial, v. 6, p. 436-439.

DeVries, T.J. 2007. Cenozoic Turritellidae (Gastropoda) from southern Peru. Journal of Paleontology, v. 81, p. 331-351.

DeVries, T.J. 2016. Fossil Cenozoic crassatelline bivalves from Peru: New species and generic insights. Acta Palaeontologica Polonica, v. 61(3), p. 661-688.

DeVries, T.J. (in press). Eocene stratigraphy and depositional history near Puerto Caballas (East Pisco Basin, Peru). Sociedad Geológica del Perú, Volumen Especial.

DeVries, T.J., Narváez, Y., Sanfilippo, A., Malumian, N., Tapia, P. 2006. New microfossil evidence for a late Eocene age of the Otuma Formation (southern Peru). XIII Congreso Peruano de Geología, Lima, Peru, October, 2006. Sociedad Geológica del Perú, Publicación Especial, v. 7, p. 615-618.

Dunbar, R.B., Marty, R.C., Baker, P.A. 1990. Cenozoic marine sedimentation in the Sechura and Pisco basins, Peru. Palaeogeography, Palaeoclimatology, Palaeoecology, v. 77, p. 235-261.

Dworschak, P.C., Rodrigues, S. de A. 1997. A modern analogue for the trace fossil *Gyrolithes*: Burrows of the thalassinidean shrimp *Axianassa australis*. Lethaia, v. 30, p. 41-52.

Feldpausch, T.R., Banin, L., Phillips, O.L., et al. 2011. Height-diameter allometry of tropical forest trees. Biogeosciences, v. 8, p. 1081-1106.

Fenner, J. 1985. Late Cretaceous to Oligocene planktonic diatoms. *In*: Plankton Stratigraphy, Bolli, H.M., Saunders, J.B., Perch-Nilsen, K. (eds.), Cambridge University Press, Cambridge, England, p. 713-762.

Galloway, W.E. 1989. Genetic stratigraphic sequences in basin analysis, I. Architecture and genesis of flooding-surface bounded depositional units. American Association of Petroleum Geologists (AAPG) Bulletin, v. 73, p. 125-142.

Glenn, C.R., Arthur, M.A., Resig, J.M., Burnett, W.C., Dean, W.E., Jahnke, R.A. 1994. Are modern and ancient phosphorites really so different? *In*: Siliceous, Phosphatic and Glauconitic Sediments of the Tertiary and Mesozoic, Iijima, A., Abed, A.M.,, Garrison, R.E. (eds.), VSP International Science Publishers, Zeist, The Netherlands, p. 159-188.

Glezer, S.I., Makarova, I.V., Moiseeva, A.I., Nikolaev, V.A. 1992. The diatoms of the U.S.S.R. fossil and Recent. Volume 2, part 2: Stephanodiscaceae, Ectodictyonaceae, Paraliaceae, Radialiplicataceae, Pseudopodosiraceae, Trochosiraceae, Melosiraceae, Aulacosiraceae. NAUKA, St. Petersburg, Russia, 128 p.

Gombos, Jr., A.M., Ciesielski, P.F. 1983. Late Eocene to early Miocene diatoms from the southwest Atlantic. *In*: Initial Reports of the Deep Sea Drilling Project, September, 1983, Ludwig, W.J., Krasheninikov, V.A., Basov, I.A., et al., Texas A&M University, Ocean Drilling Program, College Station, Texas, USA, v. 71, part 2, p. 583-634.

Hampel, A. 2002. The migration history of the Nazca Ridge along the Peruvian active margin: a re-evaluation. Earth and Planetary Science Letters, v. 203, p. 665-679.

Hanna, G.D., Israelsky, M.C. 1925. Contribution to the Tertiary paleontology of Peru. Proceedings of the Califorina Academy of Sciences, fourth series, v. 14, p. 37-75.

Higley, D.K. 2004. The Talara Basin Province of northwestern Peru: Cretaceous-Tertiary total petroleum systems. United States Geological Survey Bulletin, v. 2206-A, 20 p. Version 1.0. http://pubs.usgs.gov/bul/2206/A/.

Houben, A.J.P., van Mourik, C.A., Montanari, A. 2012. The Eocene-Oligocene transition: Changes in sea level, temperature, or both? Palaeogeography, Palaeoclimatology, Paleoecology, v. 335-336, p. 75-83.

Huber, B.T., Quillévéré, F. 2005, Revised Paleogene planktonic foraminiferal biozonation for the Austral Realm. Journal of Foraminiferal Research, v. 35, p. 299-314.

Ibaraki, M. 1993. Eocene to early Miocene planktonic foraminifera from the south of Paracas, central Peru. Report of the Faculty of Sciences, Shizuoka University, v. 27, p. 77-93.

Ksepka, D.T., Clarke, J.A. 2010. The basal penguin (Aves: Sphenisciformes) *Perudyptes devriesi* and a phylogenetic evaluation of the penguin fossil record. Bulletin of the American Museum of Natural History, v. 337, 77 p.

Lear, C.H., Bailey, T.R., Pearson, P.N., Coxall, H.K., Rosenthal,

Y. 2008. Cooling and ice growth across the Eocene–Oligocene transition. Geology, v. 36, p. 251-254.

León, W., Rosell, W., Aleman, A., Torres, V., Cruz, O. de la. 2008. Estratigrafía, sedimentología, y evolución tectónica de la Cuenca Pisco Oriental. Instituto Geológico Minero y Metalúrgico (INGEMMET), Estudios Regionales, Serie D, Boletín, v. 27, 154 p.

Lisson, C.I. 1925. Algunos fósiles de Perú. Boletín de la Sociedad Geológica del Perú, v. 1, p. 23-30.

Macharé, J. 1987. La marge continentale du Perou: Regimes tectoniques et sedimentaires cenozoiques de I'avant-arc des Andes centrales. PhD dissertation, Université de Paris XI, Orsay, France, 391 p.

Macharé, J., Fourtanier, E. 1987. Datation des formations tertiares du bassin de Pisco (Pérou) à partir d'associations de diatomé. Comptes Rendus de l'Académie des Sciences, Paris, Series II, v. 305, p. 407-412.

Macharé L., J., Ortlieb, L. 1992. Plio-Quaternary vertical motions and the subduction of the Nazca Ridge, central coast of Peru. Tectonophysics, v. 205, p. 97-108.

Martinez-Caceres, M., Muizon, C. de. 2011. A new basilosaurid (Cetacea, Pelagiceti) from the late Eocene to early Oligocene Otuma Formation of Peru. Comptes Rendus Palevol, v. 10, p. 517-526.

Martinez-Carbrera, H.I., Estrada-Ruiz, E., Castañeda-Posadas, C., Woodcock, D. 2012. Wood specific gravity estimation based on wood anatomical traits: Inference of key ecological characteristics in fossil assemblages. Review of Palaeobotany and Palynology, v. 187, p. 1-10.

Miller, K.G., Browning, J.V., Aubry, M.-P., Wade, B.S., Katz, M.E., Kulpecz, A.A., Wright, J.D. 2008. Eocene–Oligocene global climate and sea level changes: St. Stephens Quarry, Alabama. Geological Society of America (GSA) Bulletin, v. 120, p. 34–53.

Miller, K.G., Wright, J.D., Browning, J.V. 2005. Visions of ice sheets in a greenhouse world. Marine Geology, v. 217, p. 215-231.

Mitchum, Jr., R.M., Vail, P.R., Thompson, III, S. 1977. Seismic stratigraphy and global changes of sea-level, part 2: the depositional sequence as a basic unit for stratigraphic analysis. *In*: Seismic Stratigraphy – Applications to Hydrocarbon Exploration, Payton, C. E. (ed.). American Association of Petroleum Geologists (AAPG) Memoir, v. 26, p. 53-62.

Murphy, A.M., Salvador, A. 2016. Stratigraphic guide. International Commission on Stratigraphy (ICS). stratigraphy.org/upload/bak/litho.htm.

Narvaez, Y., Pardo A., A. 2009. Nannofossil biostratigraphy of Eocene strata in the Talara Basin, Peru. SEPM Special Publication, v. 93, p. 287-291.

Newell, N.D. 1956. Reconocimiento geológico de la región Pisco-Nazca. Boletín de la Sociedad Geológica del Perú, v. 30, p. 261-295.

Nielsen, S.N., DeVries, T.J. 2002. Tertiary Xenophoridae of western South America. The Nautilus, v. 116, p. 71-78.

Nigrini, C., Sanfilippo, A. 2001. Cenozoic radiolarian stratigraphy for low and middle latitudes with descriptions of biomarkers and stratigraphically useful species. ODP Technical Note, v. 27 [Online]. <http://www.odp.tamu.edu/publications/tnotes/ tn27/ index.html>. [Cited 2016-05-22]

Olsson, A.A. 1928. Contributions to the Tertiary paleontology of northern Peru. Part 1, Eocene Mollusca and Brachiopoda. Bulletins of American Paleontology, v. 14, 155 p.

Olsson, A.A. 1930. Contributions to the Tertiary paleontology of northern Peru. Part 3, Eocene Mollusca. Bulletins of American Paleontology, v. 17, 73 p.

Olsson, A.A. 1931. Contributions to the Tertiary paleontology of northern Peru. Part 4, The Peruvian Oligocene. Bulletins of American Paleontology, v. 17, 124 p.

Pearson, P.N., Olsson, R.K., Hemleben, C., Huber, B.T., Berggren, W.A. 2006. Atlas of Eocene planktonic foraminifera. Cushman Foundation for Foraminiferal Research, Special Publication, v. 41, 513 p.

Portugal, F. de, Sousa, S.T. de, Lewis, G.P., Hawkins, J.A. 2010. A revision of the South American genus *Apuleia* (Leguminosae, Cassieae). Kew Bulletin, v. 65, p. 225-232.

Pujana, R.R., Martínez, L.C.A., Brea, M. 2011. El registro de maderas fósiles de Leguminosae de Sudamérica. Revista del Museo Argentino de Ciencias Naturales (new series), v. 13, p. 183-194.

Ramsey, A.T.S., Baldauf, J.G. 1999. A reassessment of Southern Ocean biochronolgy. Geological Society of London Memoir, v. 18, 122 p.

Riascos, J.M., Heilmayer, O., Laudien, J. 2008. Population dynamics of the tropical bivalve *Cardita affinis* from Málaga Bay, Colombian Pacific related to La Niña 1999-2000. Helgoland Marine Research, v. 62, Supplement 1, p. S63-S71.

Rich, P.M., Helenurm, K., Kearns, D., Morse, S.R., Palmer, M.W., Short, L. 1986. Height and stem diameter relationships for dicotyledonous trees and arborescent palms of Costa Rican tropical wet forest. Bulletin of the Torrey Botanical Club, v. 113, p. 241-246.

Rivera, R. 1957. Moluscos fósiles de la Formación Paracas, departamento de Ica. Boletín de la Sociedad Geológica del Perú, v. 32, p. 165-220.

Saillard, M., Hall, S.R., Audin, L., Farber, D.L., Regard, V., Hérail, G. 2011. Andean coastal uplift and active tectonics in southern Peru: ^{10}Be surface exposure dating of differentially uplifted marine terrace sequences (San Juan de Marcona, ~15.4°S). Geomorphology, v. 128, p. 178-190.

Salas, R., DeVries, T., Urbina, M., García, A., Pujos, F., Aguirre, M. 2004. Los vertebrados de los humedales Pleistocénicos de Aguada de Lomas y Sacaco (Arequipa, Perú): Interpretaciones paleoecológicas. XII Congreso Peruano de Geología, Lima, Peru, October, 2004. Sociedad Geológica del Perú, Resúmenes Extendidos, Publicación Especial, v. 6, p. 529-532.

Sanfilippo, A., Nigrini, C. 1998. Code numbers for Cenozoic low latitude radiolarian biostratigraphic zones and GPTS conversion tables. Marine Micropaleontology, v. 33, p. 109-156.

Sébrier, M., Soler, P. 1991. Tectonics and magmatism in the Peruvian Andes from late Oligocene time to the present. In: Andean magmatism and its tectonic setting, Harmon, R.S., Rapela, C.W. (eds.), Geological Society of America Special Paper, v. 265, p. 259-278.

Stock, C.E. 1990. Tertiary geology of the Quebrada Huaricangana area, East Pisco Basin, southern Peru: Late

Paleogene to Neogene transgressive sedimentation within a forearc basin. Masters thesis, Rice University, Houston, Texas, 228 p.
Suess, E., Kulm, L.D., Killingley, J.S. 1987. Coastal upwelling and a history of organic-rich mudstone deposition off Peru. Geological Society of London Special Publication, v. 26, p. 181-197.
Suits, N.S., Arthur, M.A. 2000. Sulfur diagenesis and partitioning in Holocene Peru shelf and upper slope sediments. Chemical Geology, v. 163, p. 219-234.
Woods, H. 1922. Mollusca from Eocene and Miocene deposits of Peru. *In*: Geology of the Tertiary and Quaternary Periods in the northern part of Peru, Bosworth, T.O., Macmillan, London, England, p. 51-113.
Young, J.R., Bown P.R., Lees J.A. (eds). 2016. Nannotax3 website. International Nannoplankton Association. 8 Aug. 2016. URL: http://ina.tmsoc.org/Nannotax3
Zachos, J.C., Dickens, G.R., Zeebe, R.E. 2008. An early Cenozoic perspective on greenhouse warming and carbon-cycle dynamics. Nature, v. 451, p. 279-283.

Table I.
Selected fossil marine mollusks from the Pisco and Talara basins. Sources include Olsson (1928, 1930, 1931), Rivera (1957), and DeVries (1998, 2004).

Appendix
Latitude and longitude for localities of DeVries ("DV") and José Macharé ("xxJM"). See Macharé and Fourtanier (1987) for selected Macharé localities.

Locality number	Latitude	Longitude
80JM 014	14°52'S	75°26'W
83JM 021	14°52½'S	75°25½'W
83JM 062	Macharé and Fourtanier, 1987	
83JM 104	13°59'S	76°10'W
86JM 023	Macharé and Fourtanier, 1987	
86JM 060	Macharé and Fourtanier, 1987	
DV 404	13°57’34”S	76°12’34”W
DV 405	13°57’08”S	76°11’59”W
DV 415	13°57’43”S	76°11’47”W
DV 483	14°40’32”S	75°41’06”W
DV 484	14°35'38"S	75°40'10"W
DV 502	13°48'15"S	76°20'43"W
DV 508	14°38'44"S	75°38'12"W
DV 509	14°39’50”S	75°37’56”W
DV 511	15°16'20"S	75°04'04"W
DV 544	14°39’48”S	75°37’57”W
DV 546	14°39’34”S	75°38’02”W
DV 590	14°40’05”S	75°41’18”W
DV 591	14°40’28”S	75°41’03”W
DV 631	14°09’48”S	76°09’03”W
DV 632	14°11’21”S	76°08’22”W
DV 818	13°52'14"S	76°16'04"W
DV 828	13°50'02"S	76°22'16"W
DV 839	13°56’15”S	76°17’03”W
DV 842	13°58’35”S	76°13’47”W
DV 936	13°53’44”S	76°15’53”W
DV 1028	15°39'23"S	74°35'29"W
DV 1112	14°06’08”S	76°11’32”W
DV 1122	14°06’17”S	76°11’29”W
DV 1123	14°06’25”S	76°11’08”W
DV 1134	14°15'15"S	76°01'40"W
DV 1135	14°19'24"S	76°02'22"W
DV 1136	14°21’00”S	76°02’25”W
DV 1142	13°58’01”S	76°13’12”W
DV 1143	13°57’54”S	76°13’03”W
DV 1144	13°57’48”S	76°12’53”W
DV 1145	13°57’56”S	76°12’56”W
DV 1146	13°58’13”S	76°12’20”W
DV 1148	13°58’17”S	76°11’58”W
DV 1149	13°58’00”S	76°12’20”W
DV 1150	13°57’51”S	76°12’16”W
DV 1151	13°57’03”S	76°13’06”W
DV 1152	13°57’17”S	76°12’58”W
DV 1153	13°57’26”S	76°12’53”W
DV 1154	13°56'39"S	76°11'53"W
DV 1160	13°57’31”S	76°12’25”W
DV 1161	13°57’24”S	76°12’26”W
DV 1171	14°08’41”S	76°11’27”W
DV 1172	14°08’29”S	76°10’55”W
DV 1173	14°08’29”S	76°10’53”W
DV 1220	14°08’24”S	76°10’41”W
DV 1221	14°08’21”S	76°10’20”W
DV 1222	14°08’24”S	76°10’17”W
DV 1222a	14°07’50”S	76°10’18”W
DV 1402	13°56'46"S	76°11'36"W
DV 1441	14°29’02”S	75°57’19”W
DV 1442	14°28’59”S	75°57’05”W
DV 1443	14°28’49”S	75°57’10”W
DV 1444	14°28’42”S	75°57’10”W
DV 1445	14°20’50”S	76°02’43”W
DV 1456	14°51’21”S	75°25’47”W
DV 1457	14°53’54”S	75°26’07”W
DV 1616	14°41’58”S	75°35’28”W
DV 1618	14°42’06”S	75°35’31”W
DV 1619	14°42’20”S	75°35’30”W
DV 1716	14°37’22”S	75°35’50”W
DV 1727	14°37’49”S	75°35’49”W
DV 1730	14°34’25”S	75°54’05”W
DV 1731	14°34’07”S	75°54’04”W
DV 1732	14°34’38”S	75°51’37”W
DV 1734	14°33’01”S	75°54’33”W
DV 1812	14°40’08”S	75°37’54”W
DV 1813	14°38’56”S	75°38’17”W
DV 1815	14°11’20”S	76°08’25”W
DV 1819	14°08’40”S	76°10’27”W
DV 1901	14°40’11”S	75°38’04”W
DV 1902	14°40’00”S	75°37’42”W
DV 1903	14°39'49"S	75°37'46"W
DV 1904	14°39'50"S	75°37'49"W
DV 1906	14°38’58”S	75°38’57”W
DV 1913	14°08'29"S	76°10'54"W
DV 1965	14°51’56”S	75°25’07”W
DV 2036	13°55’41”S	76°17’05”W
DV 2037	13°55’11”S	76°17’05”W
DV 2038	13°56’22”S	76°16’56”W
DV 2039	13°56’25”S	76°16’47”W
DV 2040	13°55’40”S	76°16’00”W
DV 2041	13°55’49”S	76°16’56”W
DV 2042	13°55’48”S	76°16’55”W

DV 2043	13°55’39”S	76°16’52”W
DV 2044	13°55’37”S	76°16’51”W
DV 2045	13°55’25”S	76°16’50”W
DV 2046	13°55’17”S	76°16’59”W
DV 2213	14°33’46”S	75°53’09”W
DV 2219	14°34’10”S	75°53’38”W
DV 2226	14°40’18”S	75°41’31”W
DV 2247	14°18'45"S	75°57'15"W
DV 2259	14°11’27”S	76°08’27”W
DV 2260	14°11’26”S	76°08’26”W
DV 2262	14°34’13”S	75°53’35”W
DV 3013a	14°08’54”S	76°10’09”W
DV 3015	14°08’54”S	76°10’03”W
DV 3017	14°06’32”S	76°10’44”W
DV 3022	14°24’57”S	75°55’13”W
DV 3025	14°28’14”S	75°56’29”W
DV 3026	14°28’11”S	75°56’30”W
DV 3026a	14°27’45”S	75°56’37”W
DV 3028	14°28’56”S	75°57’09”W
DV 3029	14°28’56”S	75°57’08”W
DV 3030	14°28’07”S	75°55’14”W
DV 3036	14°16'29"S	75°57'13"W
DV 3059	14°34’13”S	75°53’37”W
DV 3060	14°34’18”S	75°53’29”W
DV 3063	14°34'15"S	75°53'41"W
DV 3065	14°34’24”S	75°53’47”W
DV 3066	14°34’21”S	75°54’04”W
DV 3067	14°34’25”S	75°54’14”W
DV 3069	14°34’22”S	75°52’21”W
DV 3071	14°34’57”S	75°52’08”W
DV 3072	14°34’09”S	75°52’47”W
DV 3076	14°32’59”S	75°54’37”W
DV 3089	14°34’02”S	75°53’48”W
DV 3090	14°39’55”S	75°53’42”W
DV 3091	14°33’46”S	75°53’45”W
DV 3092	14°33’48”S	75°53’32”W
DV 3093	14°33’51”S	75°53’28”W
DV 4005	14°08’10”S	76°10’09”W
DV 4022	14°40’47”S	75°36’32”W
DV 4028	14°40’14”S	75°37’59”W
DV 4031	14°39’02”S	75°39’54”W
DV 4032	14°39’18”S	75°38’32”W
DV 4033	14°39’44”S	75°39’59”W
DV 4042	14°23'02"S	75°54'00"W
DV 4066	14°21’49”S	75°54’23”W
DV 5002	14°09'59"S	76°04'44"W
DV 5023	14°09'55"S	76°08'34"W
DV 5080	14°38’50”S	75°35’46”W
DV 5082	14°38’36”S	75°35’57”W
DV 5083	14°38’39”S	75°35’52”W
DV 5084	14°25’07”S	75°55’03”W
DV 5085	14°24’51”S	75°54’56”W
DV 5086	14°24’42”S	75°55’00”W
DV 5087	14°22'38"S	75°54'55"W
DV 5089	14°22'41"S	75°54'41"W
DV 5092	14°22'40"S	75°54'50"W
DV 5100	14°22’38”S	75°54’53”W
DV 5101	14°25’18”S	75°54’50”W
DV 5103	14°25'22"S	75°54'04"W
DV 5104	14°25'18"S	75°53'59"W
DV 5105	14°24'53"S	75°53'42"W
DV 5106	14°24'26"S	75°53'33"W
DV 5108	14°24'13"S	75°53'29"W
DV 5109	14°25’32”S	75°57’34”W
DV 5110	14°26’12”S	75°57’09”W
DV 5111	14°26’30”S	75°56’57”W
DV 5112	14°26’33”S	75°56’53”W
DV 5118	14°25’22”S	75°54’52”W
DV 7036	14°47'27"S	75°30'34"W
DV 7092	14°21'40"S	75°54'25"W
DV 7102	14°23'54"S	75°53'39"W
DV 7117	14°24'36"S	75°54'39"W
DV 7118	14°24'25"S	75°54'35"W
DV 7119	14°24'22"S	75°54'35"W
DV 7120	14°24'22"S	75°54'51"W
DV 7121	14°24'17"S	75°54'56"W
DV 7122	14°24'12"S	75°54'56"W
DV 7126	14°50'33"S	75°29'51"W
DV 7127	14°23'00"S	75°54'53"W
DV 7129	14°23'49"S	75°55'11"W
DV 7130	14°23'42"S	75°55'07"W
DV 7135	14°47’31”S	75°30’28”W
DV 7136	14°47’29”S	75°30’34”W
DV 7137	14°47’29”S	75°30’38”W
DV 7138	14°47’25”S	75°30’02”W
DV 7140	14°47’30”S	75°29’52”W
DV 7141	14°47’28”S	75°29’50”W
DV 7142	14°47’30”S	75°29’48”W
DV 7143	14°47’22”S	75°29’50”W
DV 7144	14°47’33”S	75°29’36”W
DV 7146	14°46’58”S	75°30’18”W
DV 7160	14°38’48”S	75°35’21”W
DV 7161	14°34’08”S	75°34’25”W
DV 7162	14°38’42”S	75°34’56”W
DV 7165	14°39’08”S	75°36’17”W